Potential Protective Effects of Milk Thistle (*Silybum Marianum* L.) Seeds Against Benzo[*a*]Pyrene-Induced Hepatic and Nephritic Injuries in Rats: Biochemical and Histopathological Studies

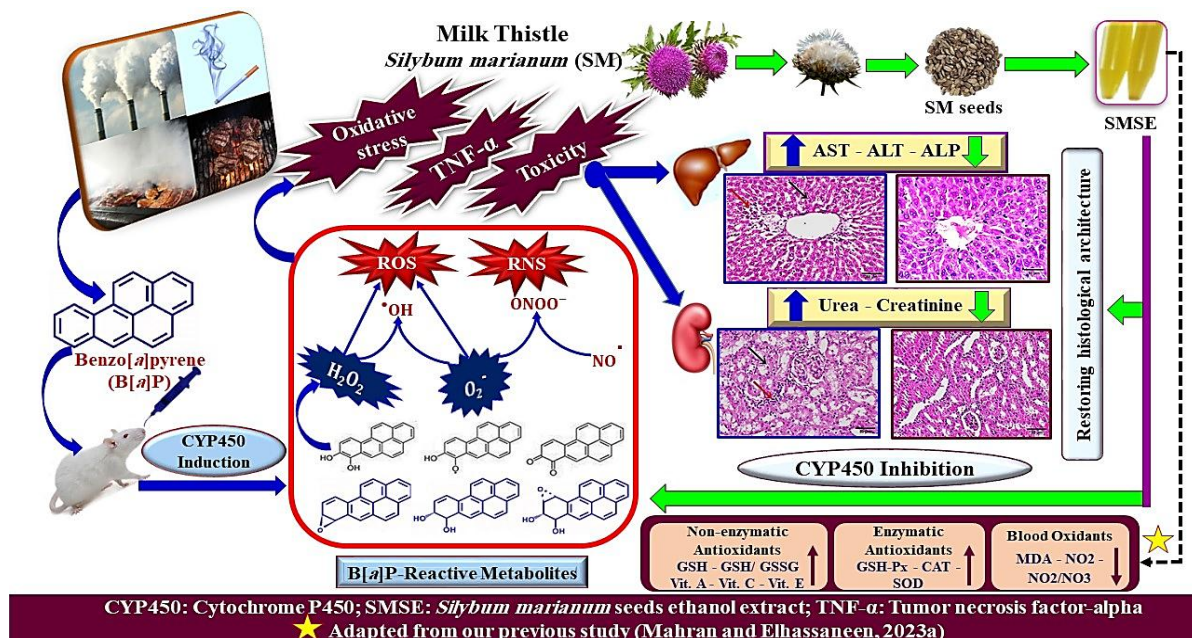Yousif A. Elhassaneen[1] and Mohamed Z. Mahran[* 1]

ABSTRACT

Benzo[*a*]pyrene (B[*a*]P), a polycyclic aromatic hydrocarbon, poses a significant threat to human health as an increasingly prevalent environmental and foodborne pollutant. Our previous study revealed that wild *Silybum marianum* seeds ethanolic extract (SMSE) attenuated B[*a*]P-induced oxidative stress and cell apoptosis in albino rats. In this work, we extended our hypothesis to investigate the potential protective effects of SMSE against hepatic and nephritic injuries induced by B[*a*]P. Thirty-six male albino rats were assigned into six groups: Group I, the control (-Ve), received 10 ml/kg/BW corn oil orally twice weekly; Group II, the control (+Ve), was given 50 mg/kg/BW of B[*a*]P in corn oil twice weekly; and Groups III, V, IV, and VI were orally administered B[*a*]P + SMSE at 200, 400, 600, and 800 mg/kg BW/day, respectively, for four weeks. B[*a*]P exposure significantly ($p \leq 0.05$) increased the relative weights of the liver (33.33%) and kidney (39.68%); cytochrome P450 (CYP450) activity, a biotransformation marker, (68.25%); tumor necrosis factor-alpha (TNF-α) levels, a pro-inflammatory mediator, (95.95%); liver enzymes activities (AST, 124.09%, ALT, 124.98%, and ALP, 128.77%); and renal function indicators (serum urea, 60.18%, and creatinine, 68.35%), accompanied by severe histopathologic changes in liver and kidney tissues compared to control (-Ve). Conversely, SMSE interventions significantly ($p \leq 0.05$) dose-dependently reduced elevated rates of these indices, while improving liver and kidney histoarchitecture. The SMSE's protective effects may result from its bioactive compounds content that regulate B[*a*]P metabolic enzymes, inhibit CYP450 activity, suppress TNF-α, and scavenge other reactive intermediates. Our results suggest SMSE as a potential natural approach to alleviating environmental pollutants' detrimental effects and deserves further research.

Keywords: *Silybum marianum*, benzo[*a*]pyrene, hepatotoxicity, nephrotoxicity, cytochrome P450, inflammatory response, histopathology

Graphical abstract

CYP450: Cytochrome P450; SMSE: *Silybum marianum* seeds ethanol extract; TNF-α: Tumor necrosis factor-alpha
★ Adapted from our previous study (Mahran and Elhassaneen, 2023a)

[1] Department of Nutrition and Food Science, Faculty of Home Economics, Menoufia University, Shebin El-Kom, Egypt
* Corresponding author: Email: mohamed.mahran@hec.menofia.edu.eg;
 ORCID ID. https://www.orcid.org/0000-0003-2480-8832

INTRODUCTION

In recent decades, significant industrial development and rapid urbanization have led to multiple human activities emitting a wide range of pollutants into the environment, such as polycyclic aromatic hydrocarbons (PAHs) (Mojiri *et al.,* 2019 and Voumik & Sultana, 2022). PAHs are a class of chemicals that are ubiquitous environmental and foodborne pollutants (Elhassaneen, 2000 and Patel *et al.,* 2020). The levels of PAHs and their potential carcinogenicity have grown considerably in recent years. The PAH family of compounds encompasses over 100 chemical species worldwide, 16 of which are of particular concern (Cui *et al.,* 2022). Benzo[*a*]pyrene (B[*a*]P), a five-ring polycyclic aromatic hydrocarbon, is the most ubiquitous PAH environmental contaminant and ranked among the top 10 pollutants identified by the United States (Amanda *et al.,* 2022 and Bukowska *et al.,* 2022). B[*a*]P has been classified as one of the most toxic carcinogens. It is further categorized as a Group 1 known carcinogen for humans by the International Agency for Research on Cancer (Vermillion Maier *et al.,* 2022).

B[*a*]P is a by-product of combustion processes. Human beings are exposed to this hazardous xenobiotic through multiple sources, such as cigarette smoke, wildfires, fossil fuel combustion, charcoal-broiled food, consumption of contaminated food and water, and inhalation of polluted air (Elhassaneen, 2004; Elhassaneen & El-Badawy, 2013; Amanda *et al.,* 2022 and Wu *et al.,* 2023). Industrial food processing, such as smoking, presents the highest B[*a*]P exposure levels. Furthermore, certain cooking practices, such as frying, roasting, and grilling meat, chicken, and fish, may also lead to elevated B[*a*]P levels (Eldaly *et al.,* 2016). The European Commission has established acceptable levels of B[*a*]P in some foodstuffs, such as smoked meat and fish products (5 µg/kg), fats and oils (2 µg/kg), and cereals (1µg/kg) (European Commission, 2005). Nonetheless, research conducted in Egypt on charcoal-grilled kebabs and kofta revealed that B[*a*]P levels were as high as 21–25 and 60–70 µg/kg, respectively (Eldaly *et al.,* 2016).

Animal studies have shown that PAHs, particularly B[*a*]P, have substantial bioaccumulation capabilities (Costa *et al.,* 2011). Owing to the lipophilic nature of B[*a*]P, it is easily absorbed through biological membranes (Jacques *et al.,* 2010), and bio-activated through the binding of the aryl hydrocarbon receptor (AhR) in the liver and subsequently metabolized to B[*a*]P-7-8-dihydrodiol 9, 10 epoxides (BPDE), an active carcinogen, through the cytochrome P450 (CYP450) enzymes. BPDE, due to its strong affinity for deoxyribonucleic acids (DNA), leads to the formation of DNA adducts (BPDE-DNA) (Elhassaneen, 1996 and Kumar *et al.,* 2017). Alternatively, the metabolism of B[*a*]P leads to the formation of B[*a*]P quinines via dihydrodiol dehydrogenases, which undergo redox cycling and trigger oxidative stress through reactive nitrogen species (RNS) and reactive oxygen species (ROS) (Mahran and Elhassaneen, 2023a). As a result, B[*a*]P exposure can cause mutations, chromosomal damage, single-strand breaks in DNA, apoptosis, as well as oxidative stress and inflammation (Rangi *et al.,* 2018). Prolonged exposure to B[*a*]P instigates the onset of cancer in various bodily organs, including the gastrointestinal system (colorectal and stomach), liver, lungs, skin, and cervix (Vermillion Maier *et al.,* 2022). Generally, xenobiotic detoxification metabolism, including B[*a*]P, comprises three distinct phases (Figure 1).
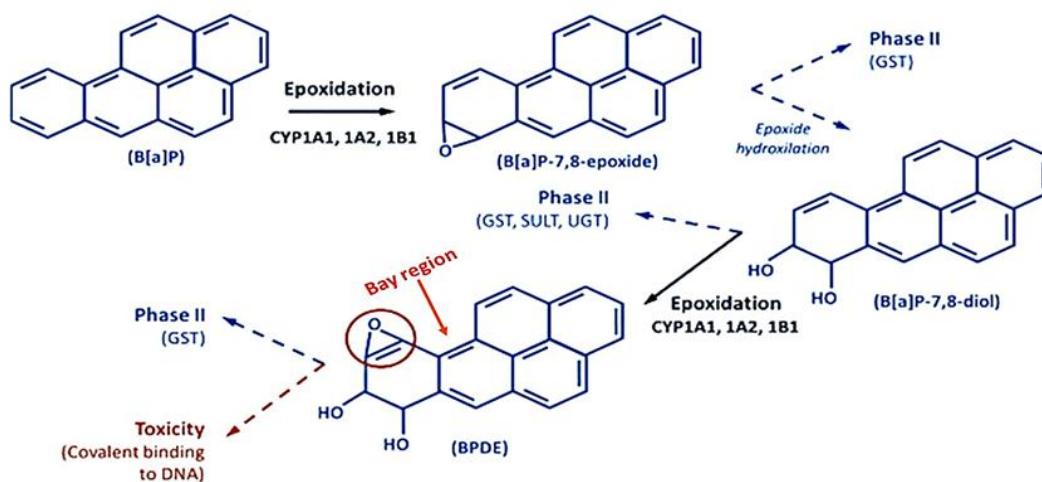

Figure 1. Bioactivation of B[*a*]P mediated by CYP450 enzymes. Adapted from Esteves *et al*. (2021)

The initial phase of this process involves the activation of phase I enzymes, including the CYP450 family 1A1 (CYP1A1), 1A2 (CYP1A2), and 1B1 (CYP1B1), which facilitate the provision of oxygen molecules to xenobiotic compounds (Tête *et al.,* 2018). Phase II enzymes such as glutathione *S*-transferase (GST), like GST alpha 1 (GSTA1) conjugate the transformed compounds to glucuronic acid, glutathione (GSH), or sulfate. During this phase, reactive substances are typically stabilized (Boei *et al.,* 2017). In the final phase (Phase III), the cells pump and eliminate conjugated xenobiotic compounds through efflux transporters like ATP-binding cassettes (ABCC1, ABCC2, and ABCC3) (Hodges and Minich, 2015).

Herbal medicine, also known as phytotherapy, is a highly prevalent complementary and alternative medicinal therapy around the world (Welz *et al.,* 2018). Milk thistle *(Silybum marianum)*, SM, is a plant of the *Silybum* genus within the *Leucanthemum* family and is native to Southern Europe, Southern Russia, Northern Africa, and Asia Minor (Soleimani *et al.,* 2019). SM is a widely recognized plant for its therapeutic and nutritional properties (Wang *et al.,* 2020). SM fruits and seeds have been used for medicinal purposes for more than 2,000 years owing to their exceptional hepatoprotective characteristics. Furthermore, within traditional Chinese medicine, SM is regarded as a herb that possesses efficacious properties for purification and detoxification (Wang *et al.,* 2020). The SM seed contains a natural complex of biological flavonolignan compounds collectively referred to as silymarin, which possesses a wide-ranging of pharmacological activities such as antioxidant, anti-bacterial, anti-viral, anti-inflammatory, anticancer, and anti-mutagenic properties (Kiruthiga *et al.,* 2015; Bektur Aykanat *et al.,* 2020; Abd Elalal *et al.,* 2022 and Mahran & Elhassaneen, 2023a). Flavonolignans are the main active constituents of SM, including silibinin, silydianine, and silychristin. Also, SM comprises a number of flavonoid compounds, including taxifolin, dihydrokaempferol, and quercetin (Stolf *et al.,* 2017). The fatty oil of SM seed contains essential phospholipids that exhibit a significant proportion of unsaturated fatty acids, specifically oleic and linoleic acids (Mahran and Elhassaneen, 2023b).

Plant-derived bioactive compounds, such as flavonoids, have recently attracted significant interest due to their ability to counteract environmental pollutants. This increased attention is primarily because individuals are frequently exposed to numerous potential contaminants and carcinogenic substances found in dietary intake, water sources, and the surrounding environment. Our recent study revealed that wild *Silybum marianum* seed ethanolic extract

(SMSE) mitigated oxidative stress and regulated liver apoptosis induced by B[*a*]P in albino rats (Mahran and Elhassaneen, 2023a). In the current study, we extended our hypothesis to explore the potential protective effects of SMSE at 200, 400, 600, and 800 mg/kg BW/day against B[*a*]P-induced hepatic and nephritic injuries in adult male albino rats.

MATERIALS AND METHODS

Materials

Chemicals

B[*a*]P ($C_{20}H_{12}$), with a purity of ≥ 96% HPLC grade, was acquired in the form of a pale yellow powder from Sigma-Aldrich (St. Louis, MO, USA). Corn oil was obtained in an oily solution as a solvent for B[*a*]P. Biochemical assay kits for evaluating liver and kidney functions were obtained from Alkan Medical Company, Cairo, Egypt. The constituents of the basal diet were provided by Morgan Chemical Company, Cairo, Egypt. All other chemicals, reagents, and solvents were of analytical grade and were procured from El-Ghomhorya Company for Trading Drugs, Chemicals, and Medical Instruments, Cairo, Egypt.

Silybum marianum seeds (SMS)

Mature and healthy wild milk thistle (*Silybum marianum*) samples were collected from Mit Ghorab Village, Senbellawein Center, Dakahlia Governorate, Egypt. Botanical authentication of the plant samples was conducted by plant taxonomists from Menoufia University's Faculty of Agriculture in Shebin El-Kom, Egypt. The seeds were carefully collected from fully matured and dried flowers. They were purified to remove foreign matter and then dried in the shade at room temperature to prevent photo-oxidation. Finally, they were kept in airtight glass containers until they were used.

Experimental animals

Ethical approval

All experiments and animal care procedures were conducted in accordance with the guidelines established by Menoufia University's Institutional Animal Care and Use Committee (IACUC), Sheibin El-Kom, Egypt. The IACUC approved all biological experiments performed in this study (Approval ID/Number: MUFHE / F / NFS / 15 / 23) as per ethical standards.

Animals (source and housing)

Experiments were conducted on 8-week-old male albino rats of the Sprague-Dawley Strain weighing (150-160 g) procured from the Laboratory Animal Unit at the College of Veterinary Medicine, Cairo University, Egypt. Animals were kept in a well-ventilated animal facility in the laboratory animals unit at the College of

Home Economics, Menoufia University, Sheibin El-Kom, Egypt. Rats were housed in groups, with a maximum of three per cage, within stainless steel cages under standard environmental conditions (the relative humidity ranged from 60-70%, the temperature 20-25°C, and a light-dark photocycle of 12/12 hours). Before experimentation, the rats were left for one week for acclimatization, provided with a basal diet, and had free access to water *ad libitum*. Meanwhile, the rats were closely monitored daily to guarantee their well-being.

Methods

Basal diet preparation

The basal diet was formulated following the modified formula of Reeves *et al*. (1993). The constituents of the basal diet, per kilogram, were comprised of: corn starch (465.692g), dextrinized corn starch (155g), sucrose (100g), casein-85% protein (140g), corn oil (40g), fiber (50g), mineral mixture (35g), vitamin mixture (10g), L-cystine (1.8g), choline bitartrate (2.5g), and tert-Butylhydroquinone (0.008g). Also, the components of minerals and vitamins mixtures were formulated based on the same reference.

SMS ethanolic extract (SMSE) preparation

SMSE was prepared by finely grinding dried SMS using an electric mixer (Moulinex Egypt, ElAraby Co., Benha, Egypt). Subsequently, a five-day extraction process in absolute ethanol (1:10 w/v) at 25°C within a flask shielded from light with intermittent shaking was conducted. Following maceration, the extract was separated from the residues through filtration using Whatman (No.1) filter paper. The filtrates were then concentrated to a consistent weight by a Rotary evaporator (Heidolph VV 2000) at low pressure, 40°C, and 50 rpm, following the methodology previously outlined by Javeed *et al*. (2022). The extract was then stored at 4°C until used.

Induction of B[*a*]P-intoxication

After a 7-day acclimation period, the rats were administered either a dose of 50 mg/kg/BW (equivalent to 1/20 of LD_{50}, as per Paltanaviciene *et al*. (2007) of B[*a*]P dissolved in 10 ml/kg/BW of corn oil through oral gavage twice weekly or a vehicle consisting of an equivalent volume of corn oil, as outlined by Dhatwalia *et al*. (2019).

Experimental design

A total of thirty-six male albino rats were randomly allocated into six groups, each consisting of six rats, and subjected to the interventions shown in Table (1). The treatments were administered via oral gavage and lasted 28 days, during which the rats were fed on the basal diet and allowed *ad libitum* access to water. Rats that underwent a B[*a*]P + SMSE treatment regimen received the B[*a*]P dose first, followed by the SMSE dose within 30 minutes. The treatment doses of SMSE were selected based on previous studies by Alaca *et al*. (2017) and Malkani *et al*. (2020). The dosages were modified weekly in line with any change in body weight to ensure an equivalent dosage per kilogram of body weight in rats throughout the entire study duration for each experimental group. The animals' final body weights were recorded at the end of the experiment. Subsequently, animals were sacrificed to collect blood samples and internal body organs (liver and kidneys).

Table 1. Experimental design to assess the potential protective effects of SMSE against hepatic and renal injuries induced by B[*a*]P*

Groups		Interventions
Group I Negative control (-Ve)	Vehicle control	10 ml/kg/BW corn oil (solvent of B[*a*]P) twice weekly.
Group II Positive control (+Ve)	B[*a*]P control	50 mg/kg/BW of B[*a*]P dissolved in corn oil twice weekly.
Group III	B[*a*]P + SMSE (200 mg/kg BW/day)	50 mg/kg/BW of B[*a*]P dissolved in corn twice weekly + 200 mg/kg BW/day of SMSE.
Group IV	B[*a*]P + SMSE (400 mg/kg BW/day)	50 mg/kg/BW of B[*a*]P dissolved in corn twice weekly + 400 mg/kg BW/day of SMSE.
Group V	B[*a*]P + SMSE (600 mg/kg BW/day)	50 mg/kg/BW of B[*a*]P dissolved in corn twice weekly + 600 mg/kg BW/day of SMSE.
Group VI	B[*a*]P + SMSE (800 mg/kg BW/day)	50 mg/kg/BW of B[*a*]P dissolved in corn twice weekly + 800 mg/kg BW/day of SMSE.

* B[*a*]P: benzo(*a*)pyrene; SMSE: *Silybum marianum* seed ethanolic extract

Blood sampling

At the end of the trial period, rats were fasted overnight and then sacrificed to collect blood samples via the abdominal aorta under sodium pentobarbital (40 mg/kg BW) anesthesia. The collected blood samples were placed in desiccated centrifuge tubes and allowed to coagulate at ambient temperature. Subsequently, centrifugation was conducted for 10 minutes at a rate of 3000 rpm to separate the serum, as per the methodology described by Parasuraman *et al.* (2010). The serum was carefully separated, placed into clean Eppendorf tubes, and kept at a temperature of -20 ℃ until subjected to biochemical analysis.

Organs harvesting

After collecting blood samples, all the experimental rats were euthanized under anesthesia. The internal body organs (the liver and both kidneys) were promptly excised, perfused with ice-cold 0.9% normal saline, dried by blotting, and weighed using an electronic balance. The relative weights of the organs, expressed as a percentage of the final body weight, were calculated according to Mee-Young *et al.* (2013). Afterwards, samples of liver and kidney tissue from each rat were conserved in separate containers containing 10% neutral buffered formalin for conducting histological examinations.

Biochemical analysis

Drug Metabolizing Enzymes (Cytochrome P450, CYP450)

CYP450 was assessed through carbon monoxide difference spectrophotometry of dithionite-reduced samples, following the method outlined by Omura and Sato (1964).

Inflammatory response biomarker (TNF-α)

TNF-α levels were determined as described by Afshari *et al.* (2005) using a sandwich enzyme-linked immunosorbent assay (ELISA), which involved the utilization of two monoclonal antibodies directed against separate antigenic determinants on rat TNF- α.

Hepatotoxicity markers

The enzyme activity of alanine aminotransferase (ALT) as well as aspartate aminotransaminase (AST) in the obtained serum samples were estimated following the modified kinetic method of Tietz (1994), while the activity of alkaline phosphatase (ALP) was evaluated using the modified kinetic method established by Vassault *et al.* (1999).

Nephrotoxicity markers

Serum urea and creatinine levels were assessed spectrophotometrically using techniques described by Tabacco *et al.* (1979) and Fabiny & Ertingshausen (1971), respectively.

Histopathological examination

In accordance with standard tissue processing procedures, formalin-fixed samples of the liver and kidney tissues of each rat were subjected to dehydration using ascending concentrations of alcohol, followed by clearance with xylene. The specimens were then embedded in paraffin wax and sectioned to a thickness of 4.5 μm using a microtome, with subsequent staining using Hematoxylin and Eosin (H&E), as outlined by Banchroft *et al.* (1996). The specimens were coded and examined under a light microscope (Olympus BX50, Tokyo, Japan) by a histopathologist to identify any characteristic histological alterations in a blinded manner to avoid any type of bias and ensure impartiality.

Statistical Analysis

All data were subjected to statistical analysis using Computer Software Package SPSS version 22. The results were presented as mean ± standard deviation (SD). One-way analysis of variance (ANOVA) was employed for statistical analysis, followed by Duncan's post-hoc test for conducting multiple comparisons between the experimental groups. A *p*-value ≤ 0.05 represents statistical significance. Furthermore, the rate of changes between the negative control group (Normal) and the positive control group (B[*a*]P control) was calculated to assess the severity of injuries caused by B[*a*]P exposure. Similarly, to further evaluate the potential protective activities of SMSE, the rate of changes between B[*a*]P control rats and those were exposed to B[*a*]P and treated with SMSE at the tested doses was computed as follows:

Rate of change compared with normal control (%) =
$$\left(\frac{B[a]P\ control\ -\ Normal\ control}{Normal\ control}\right) \times 100$$

Rate of change compared with B[*a*]P control (%) =
$$\left(\frac{Treated\ groups\ with\ SMSE\ -\ B[a]P\ control}{B[a]P\ control}\right) \times 100$$

RESULTS AND DISCUSSION

Effect of SMSE on rats' final body weight and relative organ weights

The reduction in animals' body weight indicates a deterioration in their health status. In addition to final body weight (FBW), the absolute and relative weights of the liver and kidneys and the rates of change for the relative weights in experimental groups were determined as shown in Table (2). It was observed that exposure to B[a]P led to changes in the FBW, the absolute and relative weights of the liver and kidneys in experimental animals. Despite the significant ($p \leq 0.05$) reduction in FBW in the positive control rats compared to the negative control rats, there was a noteworthy ($p \leq 0.05$) increase in the absolute and relative weights of the liver and kidneys. The rates of change for the relative weight of the liver and kidney were 33.33% and 39.68%, respectively, compared to the negative control group. These alterations may be attributed to the oxidative stress and toxicity induced by exposure to B[a]P. Such exposure imposes an extra burden on vital organs, particularly the liver and kidneys, which play a crucial role in the metabolism and excretion of B[a]P to mitigate its harmful effects, potentially leading to inflammation and enlargement of these organs. Our results are in line with Elhassaneen *et al*. (2018) and

Mahran & Elhassaneen (2023a), who found that exposure to B[a]P in male albino rats resulted in a significant reduction in the animals' body weight compared to normal control rats. Additionally, Owumi *et al*. (2021) observed that Wistar rats that were exposed to B[a]P at a dosage of 10 mg/kg for four weeks experienced a significant ($p < 0.05$) reduction in their body weight gain as compared to the control rat cohort. Meanwhile, there was an increase in the relative weights of the liver and kidneys, although this did not reach statistically significant levels. B[a]P is considered a procarcinogen, requiring metabolic activation to form reactive intermediates that induce toxic effects (Jin *et al.,* 2021). Once in the body, B[a]P tends to accumulate in various tissues, including the gastrointestinal tract, lungs, liver, kidneys, and brain (Jin *et al.,* 2021). B[a]P metabolism involves multiple enzymatic systems, contributing either to the augmentation or protection of its toxicity. The oxidative metabolism of B[a]P produces various metabolites with different reactivities, resulting in complex pathways leading to cytotoxicity, damage to macromolecules, and overall impairment of cell function and integrity (Boei *et al.,* 2017).

Table 2. Effect of SMSE on rats' final body weight and relative organ weights

	Control (-Ve)	Control (+Ve)	B[a]P treated groups with SMSE (mg/kg BW/d)			
			200	400	600	800
Final body weight (FBW; g)						
Means ± SD	216[a] ±12.37	179.5[c] ±8.43	180.25[c] ±7.4	189.5[b] ±13.19	194[b] ±15.35	206.5[a] ±9.10
% of change	0.00	-16.9	0.42	5.57	8.08	15.04
Absolute liver weight (g)						
Means ± SD	4.34 ±0.241	5.80 ±0.298	5.61 ±0.189	5.06 ±0.232	4.85 ±0.303	4.68 ±0.247
Relative liver weight (%)						
Means ± SD	2.01[c] ±0.11	2.68[a] ±0.14	2.60[a] ±0.09	2.35[b] ±0.11	2.24[b] ±0.14	2.17[bc] ±0.12
% of change	0.00	33.33	-2.99	-12.31	-16.42	-19.03
Absolute kidney weight (g)						
Means ± SD	1.35 ±0.128	1.57 ±0.036	1.51 ±0.043	1.51 ±0.041	1.42 ±0.093	1.38 ±0.056
Relative kidney weight (%)						
Means ± SD	0.63[d] ±0.065	0.88[a] ±0.026	0.84[ab] ±0.03	0.80[bc] ±0.029	0.73[c] ±0.062	0.67[d] ±0.025
% of change	0.00	39.68	-4.55	-9.09	-17.05	-23.86

Results are presented as means ± SD. The difference in mean values for groups with different superscript letters in the same row is statistically significant *(p ≤ 0.05)*. B[a]P: Benzo[a]pyrene; SMSE: *Silybum marianum* seed ethanolic extract at dosages of 200, 400, 600, and 800 mg/kg BW/day.

Conversely, oral administration of SMSE at doses of 400, 600, and 800 mg/kg/d in B[*a*]P-treated rats demonstrated a notable ($p \leq 0.05$) increase in FBW by ratios of 5.57, 8.08, and 15.04%, respectively. Additionally, there was a significant decrease in relative liver weight, with percentages of -12.31, -16.42, and -19.03%, as well as a significant decrease in relative kidney weight by -9.09, -17.05, and -23.86%, respectively, when compared to the B[*a*]P control (+Ve) group. Noteworthy, there were no significant differences in these markers between vehicle control (-Ve) rats and B[*a*]P-exposed rats treated with SMSE at 800 mg/kg/d. The observed effects may be ascribed to the bioactive compounds present in SMSE. The SM extract, known as silymarin, is an intricate mixture of natural plant-derived compounds, primarily consisting of flavonolignans, flavonoids (such as taxifolin and quercetin), and polyphenolic compounds. These constituents are known for their antioxidant properties, along with possessing various other biological characteristics (Surai, 2015). The silymarin complex comprises four flavonolignan isomers, namely silibinin, isosilibinin, silichristin, and silidianin. Among these isomers, silibinin, also known as silybin, is the most abundant and biologically active. Silibinin constitutes approximately 50-70% of the silymarin complex, while the remaining flavonolignan isomers account for around 35% of the complex (Abenavoli *et al.,* 2010). These constituents are crucial plant bioactive compounds that could potentially mitigate or prevent the adverse effects of B[*a*]P exposure through various mechanisms such as interacting with multiple transcription factors of the nuclear receptor superfamily, disrupting the activity of other transcription factors, modulating signaling pathways linked to inflammatory and oxidative stress responses, and scavenging reactive species like ROS and RNS.

Effect of SMSE on B[*a*]P-induced CYP450 activation

The first phase of the biotransformation process of B[*a*]P into B[*a*]P epoxides is mediated by the activity of cytochrome P450 (CYP450). Data in Table (3) revealed the effect of SMSE intervention on the activity of CYP450 in the negative control, positive control, and B[*a*]P + SMSE treated groups. The data demonstrated that exposure to B[*a*]P in the positive control group led to a significant ($p \leq 0.05$) increase in CYP450 levels, showing a 68.25% elevation compared to the negative control group. This finding coincides with the observations of Kiruthiga *et al.* (2015) who noted a significant increase in CYP1A1/CYP1B1 catalytic activity in adult Wistar strain rats following intraperitoneal injection of B[*a*]P at doses of (50 mg/kg/BW) twice weekly for two weeks, compared to

the vehicle control group. Furthermore, Bukowska and Duchnowicz (2022) reported that B[*a*]P has the potential to enhance AhR translocation, leading to an increase in the levels of CYP450 and other proteins involved in the metabolism of B[*a*]P. Hence, the expression of CYP1A1 is frequently used as an indicator to assess the extent of damage caused by B[*a*]P.

Phase I enzymes (CYP450) are typically the first line of defense in the body's biotransformation against potential toxic agents. These heme-thiolate monooxygenases, which are bound to microsomal membranes, are primarily located in the liver and play a crucial role in the detoxification of xenobiotics and contribute to the metabolism of numerous structurally diverse compounds (Esteves *et al.,* 2021). CYP450 enzymes' primary function is to add a reactive group, including a carboxyl, hydroxyl, or amino group, to compounds via oxidation, reduction, and/or hydrolysis processes. However, the biotransformation mediated by CYP enzymes can cause oxidative damage inside biological systems due to the conversion of environmental chemicals to reactive electrophilic species or carcinogenic substances, which is commonly referred to as "lethal synthesis" or bioactivation (Hodges & Minich, 2015 and Esteves *et al.,* 2021). Once B[*a*]P is absorbed into the gastrointestinal tract, it undergoes metabolic transformation in the liver and is converted into various metabolites through the action of cytochrome P450 enzymes. In general, B[*a*]P is subject to sequential oxidation, resulting in the formation of B[*a*]P-7,8-epoxide, B[*a*]P-7,8-dihydrodiol, and B[*a*]P-7,8-dihydrodiol-9,10-epoxide (BPDE). The metabolites derived from B[*a*]P possess mutagenic and highly carcinogenic properties, particularly BPDE in this regard (Kumar *et al.,* 2017). The bay and fjord region diol epoxides (Figure 1), which are mainly produced through the carcinogen-inducible CYP1A1/CYP1B1 enzyme, are regarded as the most cytotoxic and mutagenic metabolites of B[*a*]P (Uno *et al.,* 2001). Properly speaking, B[*a*]P is considered a procarcinogen. The manifestation of its carcinogenic properties is contingent upon the activity of cytochrome P450 (CYP1A1) and (CYP1B1) detoxification enzymes, which facilitate the enzymatic transformation of B[*a*]P into BPDE (Jee *et al.,* 2020a and Abbass *et al.,* 2021). Moreover, B[*a*]P stimulates the expression of the CYP1A1 gene by activating the AhR nuclear translocation signaling pathway (Ghosh *et al.,* 2018). AhR is a ligand-activated transcription factor well recognized for mediating the toxicity and tumor-promoting effects of carcinogens such as dioxin and B[*a*]P (Murray *et al.,* 2014).

Table 3. Effect of SMSE on B[*a*]P-induced CYP450 activation

Groups	CYP450 (nmol/mg protein)	% of change
Control (-Ve)	$1.89^d \pm 0.31$	0.00
Control (+Ve)	$3.18^a \pm 0.41$	68.25
B[*a*]P + SMSE (200 mg/kg BW/day)	$3.06^a \pm 0.43$	-3.77
B[*a*]P + SMSE (400 mg/kg BW/day)	$2.95^{ab} \pm 0.24$	-7.23
B[*a*]P + SMSE (600 mg/kg BW/day)	$2.37^c \pm 0.10$	-25.47
B[*a*]P + SMSE (800 mg/kg BW/day)	$2.28^c \pm 0.20$	-28.30

Results are presented as means ± SD. The difference in mean values for groups with different superscript letters in the same column is statistically significant $(p \leq 0.05)$. B[*a*]P: Benzo[*a*]pyrene; SMSE: *Silybum marianum* seed ethanolic extract; CYP450: Cytochrome P450.

Interestingly, oral administration of SMSE at concentrations of 600 and 800 mg/kg BW/day in B[*a*]P-treated rats showed a marked $(p \leq 0.05)$ reduction in the activity of CYP450 when compared to the corresponding values in B[*a*]P-intoxicated rats without intervention. The reduction rates were -25.47 and -28.30%, respectively, compared to the positive control. On the other hand, SMSE intervention at doses of 200 and 400 mg/kg BW/day didn't reveal any significant differences. Additionally, compared to the control (+Ve), SMSE 800 mg/kg BW/day recorded the highest inhibition effect on serum CYP450 levels in B[*a*]P-treated rats. In general, it is a beneficial approach to decrease the incidence of toxification or carcinogenesis following exposure to toxic compounds or chemical carcinogens by inhibiting the activity of phase I CYP enzymes and stimulating the activity of phase II detoxification enzymes (Korobkova, 2015). According to Kiruthiga *et al.* (2015) silymarin exhibits a significant protective effect against toxicity induced by B[*a*]P in Wistar rats through inhibition of phase I (CYP1A1) detoxification enzymes and modulation of phase II conjugating enzymes. Similar findings were noted in a study conducted by Jee *et al.* (2020b), where exposure to B[*a*]P resulted in increased expression of CYP1A1 along with a decrease in the expression of GST and ABCC1. Nevertheless, when B[*a*]P was co-administered with silymarin, the expression of GST and ABCC1 was restored, while the activation of CYP1A1 decreased. These observations suggest that silymarin may play a role in reducing the metabolism of B[*a*]P and promoting the excretion of B[*a*]P metabolites through the regulation of the enzymatic activity of phase I, II, and III metabolizing enzymes. Since CYP450 is involved in B[*a*]P transformation into highly toxic and carcinogenic compounds is well-established, inhibition of CYP450 by SMSE may potentially be effective in alleviating B[*a*]P exposure-induced damages.

Effect of SMSE on B[*a*]P-induced inflammatory response biomarker (TNF-α)

Inflammation is an adaptive response to toxic stimuli. Tumor necrosis factor alpha (TNF-α) is a cytokine that exhibits a wide range of effects on different cellular entities and functions and is a key regulator of inflammatory responses. Overactivation of TNF-α can lead to the development of pathological complications. Table (4) demonstrates the effect of oral administration of SMSE on the inflammatory response biomarker, TNF-α, induced by B[*a*]P in B[*a*]P-treated rats. Compared to the vehicle control group (-Ve), the level of the pro-inflammatory cytokine TNF-α in the B[*a*]P control (+Ve) rats, which received oral doses of B[*a*]P (50 mg/kg BW/day) twice weekly for four weeks, was significantly $(p \leq 0.05)$ higher with a notable increase rate of 95.95%, indicating that B[*a*]P stimulates the initiation of inflammatory responses and the release of pro-inflammatory cytokines. This observation aligns with earlier reports suggesting that exposure to B[*a*]P induces oxidative stress and inflammation in experimental animals (Ajayi *et al.,* 2016; Shahid *et al.,* 2016a; Owumi *et al.,* 2021; Mahran & Elhassaneen, 2023a). ROS play a crucial role in the activation of various transcription factors, particularly nuclear factor kappa B (NF-κB), which triggers the release of pro-inflammatory cytokines such as TNF-α and interleukin-6 (IL-6), consequently enhancing the activation of cyclooxygenase-2 (Reuter *et al.,* 2010). Exposure to B[*a*]P can cause oxidative stress and toxification through two distinct pathways. Firstly, B[*a*]P exposure triggers the activation of the NF-κB signaling pathway. Following *in vitro* exposure of endothelial cells to B[*a*]P, there was a significant upregulation in messenger ribonucleic acid (mRNA) expression of the NF-κB subunits p65 and p50. Consequently, there was an elevation in the levels of interleukin-1 beta (IL-1β), TNF-α, and the production of ROS (Ji *et al.,* 2013). Secondly, ROS production after B[*a*]P-quinone metabolites formation. Reports indicate that excessive ROS generated during B[*a*]P metabolism results in elevated lipid peroxidation (LPO) and a drop in the antioxidant defense system. This shift in the balance forces B[*a*]P metabolism towards toxification, resulting in the generation of more reactive metabolites and DNA

Table 4. Effect of SMSE on B[*a*]P-induced inflammatory response biomarker (TNF-α)

Groups	TNF-α (ng/L) level	% of change
Control (-Ve)	$1.48^d \pm 0.31$	0.00
Control (+Ve)	$2.90^a \pm 0.17$	95.95
B[*a*]P + SMSE (200 mg/kg BW/day)	$2.71^{ab} \pm 0.26$	-6.55
B[*a*]P + SMSE (400 mg/kg BW/day)	$2.58^{ab} \pm 0.38$	-11.03
B[*a*]P + SMSE (600 mg/kg BW/day)	$2.31^{bc} \pm 0.19$	-20.34
B[*a*]P + SMSE (800 mg/kg BW/day)	$1.97^c \pm 0.12$	-32.07

Results are presented as means ± SD. The difference in mean values for groups with different superscript letters in the same column is statistically significant $(p \leq 0.05)$. B[*a*]P: Benzo[*a*]pyrene; SMSE: *Silybum marianum* seed ethanolic extract; TNF-α: Tumor necrosis factor alpha.

adducts (Jee *et al.,* 2020a and Mahran & Elhassaneen, 2023a).

Oxidative stress can, in turn, exacerbate inflammation, creating a detrimental cycle perpetuated by the stimulation of NF-κB. In this manner, the inflammatory cytokines linked to oxidative stress contribute to the deterioration of renal tissues by triggering processes like necrosis, apoptosis, and fibrosis. Furthermore, these cytokines may have a significant role in the etiology and progression of chronic kidney disease (Gyurászová *et al.,* 2020). Moreover, TNF, a cytotoxic pro-inflammatory cytokine, is believed to be involved in the onset of liver damage. The elevated levels of circulating TNF-α prompt activation of cell surface TNF-α receptors, inducing stress-related protein kinases c-Jun N-terminal kinase (JNK) and IκB kinase (IKK). This cascade effect results in the further production of additional inflammatory cytokines (Feagins *et al.,* 2015). Hence, inhibiting TNF is considered a therapeutic approach to alleviating liver and kidney injuries.

In this context, the co-treatment of rats with B[*a*]P + SMSE (600 and 800 mg/kg BW/day) showed a marked decrease in TNF-α levels by rates of -20.34% and -32.07%, respectively, which was statistically significant $(p \leq 0.05)$ compared to the positive control group. However, the co-administration of B[*a*]P + SMSE (200 and 400 mg/kg BW/day) did not show statistically significant differences. These findings indicate a potential anti-inflammatory role for SMSE. *Silybum marianum* fruits contain diverse flavonoids. The plant's main constituent is a mixture of flavonolignans known as silymarin, known for its potent antioxidant properties. Silybin accounts for 50% of the flavonolignans in silymarin, followed by silly chrysanthemum at 20%, silydianin at 10%, and isosilibine at 5% (Khazaei *et al.,* 2022). Silybin exhibits the ability to deactivate pro-inflammatory signals associated with NF-κB activation, which is implicated in the synthesis of cytokines like TNF-α, IL-1, and IL-6 (Polyak *et al.,* 2010). This effect is attributed to its dual capability as a free radical scavenger and inhibitor of lipid peroxidation, as demonstrated in both *in vitro* and *in vivo* studies (Nencini *et al.,* 2007 and Federico *et al.,* 2015). According to Bhattacharya (2011), silymarin inhibits the inflammatory process by impeding the migration of neutrophils and Kupfer cells. Additionally, it obstructs the generation of inflammatory mediators, particularly leukotrienes and prostaglandins, by inhibiting the 5-lipoxygenase pathway. Moreover, silymarin suppresses histamine release and secretion by basophils. Furthermore, Wang *et al.* (2006) stated that taxifolin, a flavonoid found in small quantities in SMS, is capable of regulating the activation of NF-κB in rats experiencing cerebral ischemia-reperfusion injury. Their study presented evidence suggesting that taxifolin's effectiveness in modulating NF-κB activation is due to its antioxidative properties.

Oxidative stress can increase the expression of pro-inflammatory mediators, triggering an inflammatory response that exacerbates injury to the liver and kidneys. The current results indicated the anti-inflammatory property of SMSE, as evidenced by a notable reduction in the activation of the inflammatory response biomarker (TNF-α) induced by B[*a*]P, suggesting that SMSE may play a protective role against hepatic and renal injuries caused by B[*a*]P. Further biochemical and histopathological examinations were performed to verify these potential protective effects.

Effect of SMSE on B[*a*]P-induced hepatotoxicity markers

Estimating the activities of hepatic transaminases is a valuable method for evaluating the integrity of hepatocytes and the functioning of the liver. The effect of SMSE intervention on aspartate aminotransferase (AST), alanine aminotransferase (ALT), and alkaline phosphatase (ALP) activities in B[*a*]P-treated rats is illustrated in Table (5). Based on this data, it was evident that the administration of B[*a*]P resulted in a significant $(p \leq 0.05)$ increase in AST, ALT, and ALP levels in the control (+Ve) group compared to the negative one, with a remarkable increase rate of

124.09%, 124.98%, and 128.77%, respectively, which may be an indicator of hepatic dysfunction due to liver cell damage in rats that were exposed to B[*a*]P toxicity. These findings match those of Owumi *et al.* (2021), who observed a notable increase in ALT, AST, and ALP activities in Wistar rats exposed to B[*a*]P compared with the control group.

Serum transaminase estimation is beneficial in the identification of tissues/cellular injuries caused by toxic chemical exposure before conducting biopsies and histological examinations. Nevertheless, the ALT enzyme is more accurate in evaluating liver damage because AST is also elevated after muscular injury and myocardial infarction (Giannini *et al.,* 2005). Hepatic ALP is an enzyme bound to the cellular membrane, playing a pivotal role in the transportation of metabolites. The activity of this enzyme is widely considered a significant indicator of liver injury (Thapa and Walia, 2007). Elevated levels of ALP can indicate biliary system injury or obstruction of the biliary tree. Such conditions can disrupt normal blood flow to the liver (Farida *et al.,* 2012). Moreover, hepatic biosynthesis capacity can also be evaluated by assessment of AST and ALT levels, both of which are markers of hepatocyte damage. Notably, ALT serves as a specific indicator of hepatocyte necrosis. The levels of AST and ALT tend to elevate in the presence of liver necrosis caused by exposure to drugs and toxins (Roy and Bhattacharya, 2006).

The metabolic process of B[*a*]P by dihydrodiol dehydrogenases results in the production of diverse intermediary compounds that subsequently generate ROS and RNS, triggering oxidative stress. The evidence in this regard encompasses the elevation in oxidative stress biomarkers such as ROS, LPO, and protein carbonyl content (PCC) in the hepatic tissue of animals exposed to B[*a*]P, which alters the native structures and activities or functionalities of various enzymes and proteins (Rangi *et al.,* 2018). It has been documented that the metabolic process of B[*a*]P generates a substantial amount of ROS, which in turn oxidizes the reduced glutathione (GSH) into oxidized glutathione (GSSG) and exhausts the levels of GSH (Elhassaneen *et al.,* 2016; 2022 and Mahran & Elhassaneen, 2023a). This depletion of GSH not only exacerbates oxidative stress, but also leads to the subsequent deterioration of the functional and structural integrity of hepatic cells. In this context, our results revealed increased AST, ALT, and ALP activities following B[*a*]P administration, thereby suggesting hepatic injury potentially instigated by ROS, RNS, and metabolites derived from B[*a*]P. The elevated levels of these enzymes might be attributed to the release of amino acids from damaged tissue caused by B[*a*]P exposure.

On the contrary, treated groups with SMSE demonstrated the modulatory role in restoring the enzyme activities to levels close to the vehicle control. The intervention of SMSE in B[*a*]P-intoxicated rats at doses of 600 and 800 mg/kg BW/day significantly ($p \leq$ 0.05) prevented the rise of AST, ALT, and ALP activities by (-30.83 and -41.22%) for AST, (-30.30 and -44.19%) for ALT, and (-20.76 and -34.13%) for ALP, respectively, when compared to the B[*a*]P control group. Furthermore, SMSE (400 mg/kg BW/day) demonstrated marked improvement in all of these markers except for ALT. However, SMSE (200 mg/kg BW/day) did not exhibit any significant differences compared to the control (+Ve). It is worth mentioning that the most protective activity was observed in the SMSE (800 mg/kg BW/day) group, followed by SMSE (600 mg/kg BW/day).

Table 5. Effect of SMSE on B[*a*]P-induced hepatotoxicity markers

Groups	AST (U/L)	% of change	ALT (U/L)	% of change	ALP (U/L)	% of change
Control (-Ve)	62.18[e] ± 5.41	0.00	40.67[d] ± 3.08	0.00	133.80[e] ± 9.75	0.00
Control (+Ve)	139.34[a] ± 6.23	124.09	91.50[a] ± 6.62	124.98	306.09[a] ± 21.80	128.77
B[*a*]P + SMSE (200 mg/kg BW/day)	131.85[a] ± 4.44	-5.38	83.90[a] ± 4.50	-8.31	296.40[a] ± 23.96	-3.17
B[*a*]P + SMSE (400 mg/kg BW/day)	107.07[b] ± 7.81	-23.16	77.77[ab] ± 2.9	-15.01	281.39[b] ± 18.05	-8.07
B[*a*]P + SMSE (600 mg/kg BW/day)	96.38[c] ± 8.03	-30.83	63.78[b] ± 5.14	-30.30	242.56[c] ± 14.11	-20.76
B[*a*]P + SMSE (800 mg/kg BW/day)	81.91[d] ± 3.87	-41.22	51.07[c] ± 4.33	-44.19	201.61[d] ± 11.43	-34.13

Results are presented as means ± SD. The difference in mean values for groups with different superscript letters in the same column is statistically significant *(p ≤* 0.05). B[*a*]P: Benzo[*a*]pyrene; SMSE: *Silybum marianum* seed ethanolic extract; AST: Aspartate aminotransferase; ALT: Alanine aminotransferase; ALP: Alkaline phosphatase.

Multiple hepatoprotective agents, mainly plant-based substances that comprise bioactive compounds, can protect against ROS-mediated tissue damage through their antioxidant and free radical scavenging properties. In this context silymarin, a bioflavonoid, is the principal constituent of SM. In terms of its chemical composition, silymarin can be classified as a flavonolignan comprising a combination of primarily three flavonoids, namely silibinin, silydianin, and silychristin. Among these components, silibinin, constituting 70-80% of silymarin, is believed to be the most biologically active compound (Kiruthiga *et al.,* 2007). The presence of a hydroxyl group molecule in the chemical structure of silymarin is responsible for its antioxidant properties. Furthermore, the antioxidant capacity of flavonoids is enhanced by the presence of unsaturation and a 4-oxo function in the C ring (Farkas *et al.,* 2004). The relationship between the structure and antioxidant activity of flavonoid compounds has revealed that the presence of hydroxyl groups on the 3rd and 5th carbon atoms considerably enhances antioxidant activity by approximately 65%. This observation is likewise associated with silymarin because of its components, silibinin, silydianin, and silychristin, which contain hydroxyl groups on the 3rd and 5th carbon atoms (Kiruthiga *et al.,* 2007). Additionally, all of these compounds possess an extra hydroxyl group at the 7th carbon atom, which could explain the potent antioxidant properties exhibited by silymarin (Nabavi *et al.,* 2012). Silymarin protects hepatocytes through various mechanisms. It enhances the stability of membrane permeability by inhibiting lipid peroxidation. Consequently, it aids the liver in preserving its own protective antioxidant, glutathione. Silymarin stimulates the synthesis of hepatic glutathione, which is crucial for the antioxidant defense system, by improving the availability of cysteine through the regulation of sulfur-containing amino acid metabolism (Kwon *et al.,* 2013). Silymarin additionally provides protection against damage caused by toxic substances (Li *et al.,* 2012) and alleviation of hepatic steatosis and fibrosis (Ou *et al.,* 2018) through inhibition of the synthesis of IL-2, IL-4, interferon-gamma, and TNF-α, thereby downregulating the expression of inflammation-related genes and suppressing hepatic NF-κB activation. These findings suggest that SMSE may offer protection against hepatic injury induced by B[*a*]P exposure in albino rats, which was further confirmed by histopathological examination (Figure 2).

Effect of SMSE on B[*a*]P-induced nephrotoxicity markers

Kidneys are particularly susceptible to ROS attacks as they play a vital role in metabolic and filtration processes. Oxidative stress caused by ROS primarily triggers the release of an array of pro-inflammatory cytokines, which in turn leads to nephrotic inflammation and ultimately impairs renal function (Jiang *et al.,* 2017). The effect of SMSE intervention on serum urea and creatinine concentrations in B[*a*]P-treated rats is shown in Table (6). It was clear that treating rats with B[*a*]P led to a significant ($p \leq 0.05$) increase in the mean values of serum urea and creatinine compared to those in the negative control group, with a rate of increase of 60.18 and 68.35%, respectively. It is widely recognized that serum urea and creatinine levels serve as biomarkers for assessing glomerular filtration rate, which is used as an indicator in clinical research to evaluate renal function. Our histopathological examination results (Figure 3. 2a & b) showed a marked vacuolization of the epithelial lining of the renal tubules and congestion of the glomerular tufts in the kidney of intoxicated rats with B[*a*]P. These observations may indicate the presence of nephrotic glomerular dysfunction, leading to increase serum urea and creatinine concentrations in rats exposed to B[*a*]P. These results align with the findings of Khattab *et al.* (2021), who found that oral administration of B[*a*]P of 50 mg/kg BW twice a week for 28 days resulted in a highly significant elevation in serum urea and creatinine concentrations in the B[*a*]P treated rats in comparison with the normal rats. Furthermore, Sinha and Dash (2018) have demonstrated that oral administration of B[*a*]P (120 mg/kg BW) in Swiss albino mice resulted in renal damage alongside marked DNA fragmentation and alteration in DNA integrity in the kidney when compared to the control group. The increase in serum urea concentration may be attributed to excessive degradation of proteins and enzymes caused by ROS. Additionally, diminished renal function engendered retention or accumulation of urea. Accumulation of serum urea occurs when the production rate outstrips the clearance rate, indicating renal dysfunction (Sivanagi *et al.,* 2012). Moreover, an elevated serum creatinine level signifies the retention of creatinine in the bloodstream, consequent to the progressive kidney degradation caused by exposure to reactive metabolites of B[*a*]P, which readily generates free radicals (Ogbonna *et al.,* 2016).

Through the activation of AhR by CYP1A1-mediated metabolism, B[*a*]P undergoes processes that lead to the formation of B[*a*]P radical cations, subsequent free radicals generation, and the production of benzoquinones (Bukowska and Duchnowicz, 2022). These processes collectively result in oxidative damage to biomolecules. The detrimental effects of B[*a*]P are often linked to its metabolic transformations, resulting in the production of ROS and the induction of DNA

damage. These mechanisms are pivotal in understanding the toxicity associated with B[*a*]P (Bukowska and Duchnowicz, 2022). Furthermore, several studies have documented that exposure to B[*a*]P induced a significant decrease in tissue antioxidant armory activities such as superoxide dismutase (SOD), glutathione peroxidase (GSH-Px), catalase (CAT), GST, and GSH, with subsequent elevation in the levels of toxicity markers, such as lipid peroxidation (malondialdehyde, MDA), nitrite (NO_2), nitrite/nitrate (NO_2/NO_3), lactate dehydrogenase LDH, and B[*a*]P metabolizing enzymes like microsomal epoxide hydrolase (mEH) and NADPH-cytochrome P450 reductase (CYPOR) in experimental animals (Elhassaneen *et al.,* 2016; 2018; Shahid *et al.,* 2016b; Mahran *et al.,* 2018 and Mahran & Elhassaneen, 2023a). The elevation of such particular substances can potentially cause detrimental consequences for the functional and structural integrity of the tissues, inducing cellular injuries. The susceptibility of renal tissue to harm inflicted by toxins that create oxidative stress can be ascribed to the augmented metabolic state, active enzymes, and significant oxygen requirements of kidney tissue (Jiang *et al.,* 2017). Additionally, renal tissue harbors the highest concentrations of physiological markers of lipid peroxidation, which are particularly susceptible to the hazardous byproducts of B[*a*]P (Murawska-Ciałowicz *et al.,* 2011). Moreover, B[*a*]P is predominantly trapped within the kidneys, rendering them a target organ for its injurious effects (Jee *et al.,* 2020a).

In terms of our findings, as compared to the positive group, it was noted that the SMSE interventions administered at doses of 400, 600, and 800 mg/kg BW/day were capable of preventing renal injury and exhibited a significant ($p \leq 0.05$) reduction in serum urea and creatinine levels in B[*a*]P-intoxicated rats in a dose-dependent manner. These interventions effectively prevented the rise in serum urea by rates of -17.44, -21.70, and -31.22% and serum creatinine by rates of -21.80, -35.34, and -36.84%, respectively, when compared to the control (+Ve). Although the SMSE at dose of 200 mg/kg BW/day intervention partially prevented the elevation of these parameters, it did not reach statistically significant levels. Furthermore, the SMSE at dose of 800 mg/kg BW/day intervention was far superior to others in neutralizing kidney functions compared to the control (-Ve). These findings are somewhat compatible with the results obtained by Malkani *et al.* (2020), who indicated that the administration of *S. marianum* seed extract effectively protected the kidney from damage caused by vancomycin-induced oxidative stress in Swiss male albino mice.

The antioxidant enzymes serve as the defense response system against oxidative stress and counteract its detrimental effects. Studies conducted by Shahid *et al.* (2016b) and Mahran & Elhassaneen (2023a) demonstrated a notable decrease in levels of both enzymatic antioxidants (GSH-Px, CAT, and SOD) and non-enzymatic antioxidants (GSH and GSSG) following B[*a*]P administration. Additionally, there was a marked increase in the levels of MDA (Mahran and Elhassaneen 2023a). However, the administration of SMSE attenuated these changes and restored enzymatic and non-enzymatic antioxidant armories, along with exhibiting its anti-lipid peroxidative activity, as documented by Mahran and Elhassaneen (2023a). Several toxicological investigations have demonstrated evidence of the presence of AhR in renal tissues, suggesting the potential metabolic activation of B[*a*]P to reactive intermediates in the kidneys, similar to that which takes place in hepatic cells (Nanez *et al.,* 2001 and Ortiz-Delgado *et al.,* 2008). Moreover, Zhao *et al.* (2019) documented that AhR activation is implicated in renal cell carcinoma and kidney diseases. Flavonoids derived from natural sources represent the most extensive components of AhR ligands, indicating their ability to inhibit AhR transformation (Fukuda *et al.,* 2009). These might explain SMSE' protective effect against B[*a*]P-induced nephrotoxicity.

Table 6. Effect of SMSE on B[*a*]P-induced nephrotoxicity markers

Groups	Urea (mg/dl)	% of change	Creatinine (mg/dl)	% of change
Control (-Ve)	39.33[d] ± 2.21	0.00	0.79[c] ± 0.04	0.00
Control (+Ve)	63.00[a] ± 4.51	60.18	1.33[a] ± 0.1	68.35
B[*a*]P + SMSE (200 mg/kg BW/day)	59.33[ab] ± 3.79	-5.83	1.20[ab] ± 0.06	-9.77
B[*a*]P + SMSE (400 mg/kg BW/day)	52.01[bc] ± 3.61	-17.44	1.04[b] ± 0.05	-21.80
B[*a*]P + SMSE (600 mg/kg BW/day)	49.33[c] ± 4.21	-21.70	0.86[c] ± 0.04	-35.34
B[*a*]P + SMSE (800 mg/kg BW/day)	43.33[cd] ± 2.59	-31.22	0.84[c] ± 0.04	-36.84

Results are presented as means ± SD. The difference in mean values for groups with different superscript letters in the same column is statistically significant, ($p \leq 0.05$). B[*a*]P: Benzo[*a*]pyrene; SMSE: *Silybum marianum* seed ethanolic extract.

Histopathological examinations

Effect of SMSE on B[*a*]P-induced histological alterations in liver tissues

Histopathological examination was performed on liver tissues to further investigate the potential protective effects of SMSE against B[*a*]P-induced hepatic injury. Figure (2) illustrates photomicrographs of liver cells from all experimental groups. The examination revealed that liver sections from the negative control group demonstrated the normal histoarchitecture of the hepatic lobule. In contrast, the liver tissue of rats that were exposed to B[*a*]P exhibited severe histopathological changes that involved vacuolar degeneration of hepatocytes, focal hepatocellular necrosis associated with inflammatory cells infiltration, activation of Kupffer cells, fibroplasia in the portal triad, and appearance of newly formed bile ductules. Consistent with our findings, Kiruthiga *et al.* (2015) demonstrated that the liver sections of rats that received B[*a*]P at a dosage of 50 mg/kg/body weight showed hepatic necrosis, hepatocyte degeneration, loss of hepatic plate architecture, and infiltration of mononuclear cells. Moreover, Rangi *et al.* (2018) observed that the hepatocytes experience apoptosis, characterized by pyknotic nuclei, along with the manifestation of ballooning degeneration, which was evident through the swollen wispy cytosol and the presence of eosinophilic councilman bodies in B[*a*]P-treated rats.

Oxidative stress has been regarded as a co-pathological mechanism that triggers both the onset and progression of liver damage (Li *et al.,* 2015). The liver is highly vulnerable to ROS attacks (Sánchez-Valle *et al.,* 2012). The liver encounters injury due to oxidative stress, mainly in its parenchymal cells. Additionally, Kupffer cells, endothelial cells, and stellate cells are thought to be more susceptible to exposure or sensitivity to molecules associated with oxidative stress (Sánchez-Valle *et al.,* 2012). In response to oxidative stress, a diversity of cytokines such as TNF-α may be generated within Kupffer cells, thereby potentially augmenting inflammation and apoptosis. In the case of hepatic stellate cells, LPO resulting from oxidative stress stimulates cell proliferation and collagen synthesis (Cichoż-Lach and Michalak, 2014). Hajam *et al.* (2022) reported that ROS instigates damage to the membranes of hepatocytes, resulting in deuteriation, which causes collagen accumulation in the hepatocytes. This accumulation leads to the development of liver fibrosis and ultimately results in liver cirrhosis. Additionally, hepatic cells experience lipoapoptosis due to incomplete biomolecule oxidation and trigger immune reactions in the liver.

In contrast, in B[*a*]P-intoxicated rats treated with SMSE, liver tissues showed varying degrees of improvement in histopathological changes depending on SMSE dose, indicating that the degenerative alterations were mitigated and the liver's histological architecture was improved significantly. Among the tested interventions, SMSE at 800 mg/kg BW/day was the most effective (Figure 2.6. a and b). It exhibited only slight hepatocellular vacuolar degeneration in some hepatocytes within specific liver sections, while others displayed a normal histological architecture of the hepatic lobule. These improvements in liver tissue histoarchitecture may be attributed to the antioxidant properties of SMSE. Silymarin, an extract from the SM seeds, can diminish oxidative stress and subsequent cytotoxicity, thus protecting intact hepatocytes or cells that have not yet sustained irreversible damage. Silymarin acts as a scavenger of free radicals and regulates the activity of enzymes linked to the progression of cellular injury, fibrosis, and cirrhosis (Gillessen and Schmidt, 2020).
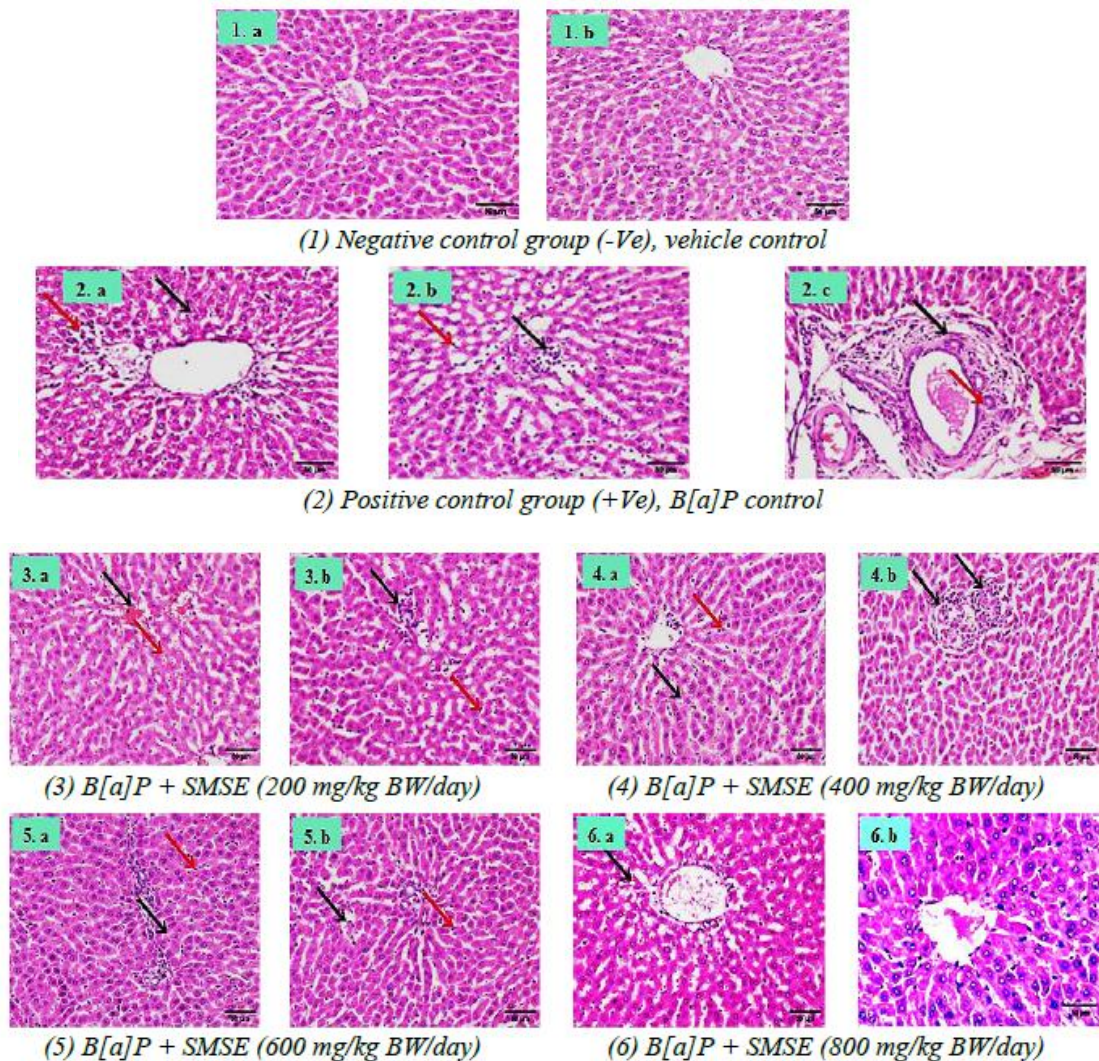
Figure 2. Effect of SMSE on B[*a*]P-induced histological alterations in liver tissues

(1): Vehicle control group (-Ve); normal histoarchitecture of hepatic lobules (1. a & b). **(2):** B[*a*]P control (+Ve); vacuolar degeneration of hepatocytes (black arrow) and focal hepatocellular necrosis associated with inflammatory cells infiltration (red arrow) (2. a), activation of Kupffer cells (red arrow) and also focal hepatocellular necrosis associated with inflammatory cells infiltration (black arrow), (2. b), and fibroplasia in the portal triad (black arrow) and appearance of newly formed bile ductules (red arrow), (2. c). **(3):** B[*a*]P + SMSE (200 mg/kg BW/day*)*; congestion of the central vein (black arrow) and hepatic sinusoids (3. a); and small focal hepatocellular necrosis associated with inflammatory cells infiltration (black arrow) and activation of Kupffer cells (red arrow), (3. b). **(4):** B[*a*]P + SMSE (400 mg/kg BW/day); hepatocellular vacuolar degeneration of some hepatocytes (black arrow) and Kupffer cells proliferation (red arrow), (4. a) and focal hepatocellular necrosis associated with inflammatory cells infiltration (4. b). **(5):** B[*a*]P + SMSE (600 mg/kg BW/day); hepatocellular vacuolar degeneration of some hepatocytes (black arrow) and Kupffer cells proliferation (red arrow), (5. a & b). **(6):** B[*a*]P + SMSE (800 mg/kg BW/day); slight hepatocellular vacuolar degeneration of some hepatocytes (6. a), the other sections exhibited the normal histological structure of the hepatic lobule (6. b). (H & E X 400, scale bar 50μm).

Our findings may corroborated by previous studies, which have proposed that silymarin exhibits promising antifibrotic activity in experimental liver injury due to its composition of silybin, silychristin, silydianin, and isosilybin. The potential hepatoprotective mechanisms of silymarin may involve inhibition of LPO, elevation of intracellular GSH content, regulation of membrane permeability, enhancement of membrane stability in the face of xenobiotic damage, and hindrance of stellate hepatocyte transformation into myofibroblasts. This transformation is accountable for collagen fiber deposition, which can lead to cirrhosis (Fried *et al.,* 2012; Ogbonna *et al.,* 2016 and Mahran & Elhassaneen, 2023a). Moreover, silymarin has the potential to

alleviate hepatic inflammation in experimental animals by inhibiting the lipo-oxygenase cycle and reducing leukotrienes and Kupffer cell function (Ross, 2008).

These findings indicated that SMSE effectively normalized liver function and partially repaired hepatic tissue damage. The protective effect of SMSE might be more pronounced at higher dosages or longer treatment durations. Consequently, it can be concluded that SMSE has the potential to protect against hepatic injuries induced by B[*a*]P in albino rats by mitigating the oxidative stress caused by B[*a*]P and its toxic reactive metabolites.

Effect of SMSE on B[*a*]P-induced histological alterations in kidney tissues

Photomicrographs in Figure (3) illustrate kidney tissue samples from experimental groups. Microscopically, examination of the kidney tissues of rats from the control (-Ve) group displayed normal histological architecture of renal parenchyma. Conversely, the kidneys of rats from the control (+Ve) group exhibited marked vacuolization of epithelial lining renal tubules, congestion of the glomerular tufts,

and intertubular inflammatory cell infiltration. These findings are consistent with recent results from Khattab *et al*. (2021), who documented that B[*a*]P exposure at a dosage of 50 mg/kg body weight twice a week for a four-week resulted in the appearance of a variety of detrimental consequences in rats' kidney tissue. These consequences included disorganized glomeruli accompanied by congested blood capillaries. Additionally, in the majority of cases, the tubules had lost their brush border and exhibited an obstructed lumen. Furthermore, Adedara *et al*. (2015) noted that the kidneys of rats exposed to B[*a*]P exhibited multiple protein casts within the tubular lumen, indicating nephrotic glomerular dysfunction. In contrast, Owumi *et al*. (2021) reported that administration of B[*a*]P at a dosage of 10 mg/kg per day for four weeks had no impact on renal histology. The variations in the reported findings may be attributed to the different dosages of B[*a*]P used in these studies. In this context, we postulate that all the observed kidney abnormalities could potentially be associated with the detrimental effects of oxidative stress exerted by B[*a*]P.
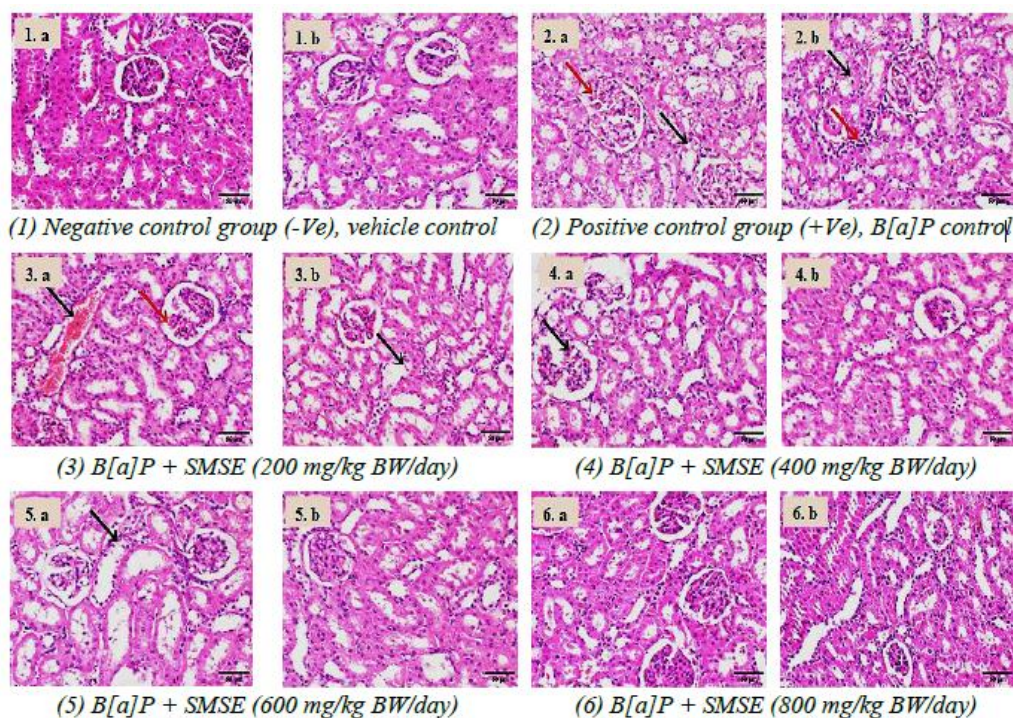

(1) Negative control group (-Ve), vehicle control   *(2) Positive control group (+Ve), B[a]P control*

(3) B[a]P + SMSE (200 mg/kg BW/day)   *(4) B[a]P + SMSE (400 mg/kg BW/day)*

(5) B[a]P + SMSE (600 mg/kg BW/day)   *(6) B[a]P + SMSE (800 mg/kg BW/day)*

Figure 3. Effect of SMSE on B[*a*]P-induced histological alterations in kidney tissues

(1): Negative control group (-Ve); normal histological structure of renal parenchyma (1. a & b). **(2):** Positive control group (+Ve); marked vacuolization of epithelial lining renal tubules, (2. a & b), (black arrow), congestion of glomerular tuft (2. a), (red arrow), and intertubular inflammatory cells infiltration, (2. b), (red arrow). **(3):** B[*a*]P + SMSE (200 mg/kg BW/day); congestion of renal blood vessels (black arrow) and glomerular tuft (red arrow), (3. a), necrosis of epithelial lining of some renal tubules (3. b). **(4):** B[*a*]P + SMSE (400 mg/kg BW/day); congestion of glomerular tuft (4. a), the other sections exhibited no histopathological alterations (4. b). **(5):** B[*a*]P + SMSE (600 mg/kg BW/day); vacuolar degeneration of the epithelial lining of some renal tubules (5. a), the other sections displayed no histopathological alterations (5. b). **(6):** B[*a*]P + SMSE (800 mg/kg BW/day); no histopathological alterations (6. a & b). (H & E X 400, scale bar 50µm).

Oxidative stress is implicated in the pathophysiology of numerous disorders that impact the renal system, including glomerular- and tubule-interstitial nephritis, renal ischemia, uremia, proteinuria, tubular necrosis, apoptosis, and renal failure (Lv *et al.,* 2018 and Hajam *et al.,* 2022). Kidneys are adversely affected by oxidative stress primarily due to the activation of inflammatory cells and pro-inflammatory cytokine production owing to ROS generation, resulting in an initial inflammatory stage (as indicated in Table 4). During this early phase, TNF-α and IL-1b play a significant role as pro-inflammatory mediators, along with NF-κB as a transcriptional factor crucial for sustaining the inflammatory process. The subsequent phase is distinguished by an increase in the production of TGF-beta, which plays a pivotal role in the synthesis of the extracellular matrix. Consequently, when kidney tissues are exposed to chronic oxidative stress stimuli, the outcome is an initial inflammatory stage, followed by excessive production of fibrotic tissue (Sun *et al.,* 2021 and Ha *et al.,* 2022). Eventually, oxidative stress aggravates progressive glomerular damage, tubular atrophy, and interstitial fibrosis, ultimately leading to a decline in renal function and renal failure (Tutun *et al.,* 2019).

Regarding our findings, the kidneys of rats from the B[*a*]P + SMSE (200 mg/kg BW/day) group showed congestion of renal blood vessels and glomerular tufts, as well as necrosis of the epithelial lining of some renal tubules. Meanwhile, certain kidney sections of rats from the B[*a*]P + SMSE (400 mg/kg BW/day) group exhibited congestion of glomerular tufts, while other sections showed no histopathological alterations. Additionally, some kidney specimens from the B[*a*]P + SMSE (600 mg/kg BW/day) group demonstrated vacuolar degeneration of the epithelial lining of some renal tubules, while others revealed no histopathological changes. It is noteworthy that no histopathological changes were observed in the rats' kidney tissues of the B[*a*]P + SMSE (800 mg/kg BW/day) treated group. These observations can be corroborated by the findings of Dumludag *et al.* (2022), who found that silymarin, an extract of *Silybum marianum* seeds, exhibited ameliorative effects on tubular necrosis, while boosting the activity of antioxidant molecules, such as GSH-Px and SOD in rats experiencing colistin-induced acute nephrotoxicity. In addition, Prabu and Muthumani (2021) documented that pathological abnormalities in the kidney, such as tubular necrosis, tubular degeneration, and tubular dilation, were significantly attenuated by silibinin administration in experimental rats exposed to arsenic-induced nephrotoxicity. The chemical constituents of milk thistle fruit include, in addition to flavonolignans, other flavonoids such as taxifolin and quercetin (Stolf *et al.,* 2017). Kim *et al.* (2021) reported that quercetin, along with its metabolite isorhamnetin, effectively inhibits the absorption of B[*a*]P by hepatic cells, inducing a noteworthy reduction in the intracellular levels of both B[*a*]P and its metabolites, exhibiting a reduction in the cytotoxicity induced by B[*a*]P. Additionally, these compounds displayed elevation levels of the gene and protein expression levels of phase I, II, and III enzymes, which play a crucial role in xenobiotic detoxification. Our results suggest that the renoprotective effect of SMSE, as further confirmed by the histopathological examination of kidney tissues, may be attributed to its potent antioxidants that effectively counteract the generation of free radicals or reactive metabolites released during B[*a*]P metabolism.

CONCLUSION

B[*a*]P, a PAH, is a ubiquitous environmental and foodborne pollutant known for its highly toxic nature and significant impact on human health. Plant-derived bioactive compounds have recently garnered substantial interest owing to their capacity to counteract pollutants. Data of this study demonstrated that exposure to B[*a*]P induced significant injuries to the liver and kidneys, leading to disruptions in biochemical markers, inflammatory responses, and substantial alterations in the histological structure of hepatic and kidney tissues in B[*a*]P-exposed rats. In contrast, oral administration of SMSE at doses of 200, 400, 600, and 800 mg/kg BW/day exhibited remarkable hepatoprotective and nephroprotective effects against B[*a*]P-induced toxicity, notably SMSE at 800 mg/kg BW/day. Moreover, SMSE interventions effectively reversed all histopathological changes to a considerable degree in a dose-dependent manner. These findings may offer new insights for developing a novel hepato-renal preventative strategy using SMSE as a dietary supplement for individuals at risk of B[*a*]P contamination.

Abbreviations

ABC: ATP-binding cassette; AhR: aryl hydrocarbon receptor; ALP: alkaline phosphatase; ALT: alanine

aminotransferase; AST: aspartate aminotransaminase; B[*a*]P: benzo[*a*]pyrene; BPDE: B[*a*]P-7-8-dihydrodiol 9, 10 epoxides; CAT: catalase; CYP450: cytochrome P450; DNA: deoxyribonucleic acids; FBW: final body weight; GPx, glutathione peroxidase; GSH: reduced glutathione; GSH-Px: glutathione peroxidase; GSH-Rd: glutathione reductase; GSSG: oxidized glutathione; GST: glutathione-*S*-transferase; IL: interleukin; LDH: lactate dehydrogenase; LPO: lipid peroxidation; MDA: malondialdehyde; mEH: microsomal epoxide hydrolase; NADPH: nicotinamide adenine dinucleotide phosphate; NF-κB: nuclear factor kappa B; PAHs: polycyclic aromatic hydrocarbons; PCC: protein carbonyl content; RNS: reactive nitrogen species; ROS: reactive oxygen species; SD: standard deviation; SM: *Silybum marianum*; SMS: *Silybum marianum* seeds; SMSE: *Silybum marianum* seed ethanolic extract; SOD: superoxide dismutase; TGF-beta: transforming growth factor-β; TNF-α: tumor necrosis factor alpha.

REFERENCE

Abbass, M., Y. Chen, V.M. Arlt and S.R. Stürzenbaum. 2021. Benzo[*a*]pyrene and Caenorhabditis elegans: defining the genotoxic potential in an organism lacking the classical CYP1A1 pathway. *Arch Toxicol*. 95:1055–69. doi: 10.1007/s00204-020-02968-z.

Abd Elalal, N.S., S.A. Elsemelawy and Y.A. Elhassaneen. 2022. Potential effects of wild milk thistle (*silybum marianum* l.) seed extract intervention on oxidative stress induced by busulfan drug in different organs of rats. *International Journal of Healthcare and Medical Sciences*, 8(3): 19-34. doi.org/10.32861/ijhms.83.19.34.

Abenavoli, L., R. Capasso, N. Milic and F. Capasso. 2010. Milk thistle in liver diseases: past, present, future. *Phytother Res*. 24(10):1423-32. doi: 10.1002/ptr.3207.

Adedara, I.A., Y.M. Daramola, J.O. Dagunduro, M.A. Aiyegbusi and E.O. Farombi. 2015. Renoprotection of Kolaviron against benzo (a) pyrene-induced renal toxicity in rats. *Ren Fail*. 37(3):497-504. doi: 10.3109/0886022X.2015.1006085.

Afshari, J.T., N. Ghomian, A. Shameli, M.T. Shakeri, M.A. Fahmidehkar, E. Mahajer, R. Khoshnavaz and M. Emadzadeh. 2005. Determination of Interleukin-6 and Tumor Necrosis Factor-alpha concentrations in Iranian-Khorasanian patients with preeclampsia. *BMC Pregnancy Childbirth*. 1;5:14. doi: 10.1186/1471-2393-5-14.

Ajayi, B.O., I.A. Adedara and E.O. Farombi. 2016. Benzo(a)pyrene induces oxidative stress, pro-inflammatory cytokines, expression of nuclear factor-kappa B and deregulation of wnt/beta-catenin signaling in colons of BALB/c mice. *Food Chem Toxicol*. 95:42-51. doi: 10.1016/j.fct.2016.06.019.

Alaca, N., D. Özbeyli, S. Uslu, H.H. Şahin, G. Yiğittürk, H. Kurtel, G. Öktem and B. Çağlayan Yeğen. 2017. Treatment with milk thistle extract (*Silybum marianum*), ursodeoxycholic acid, or their combination attenuates cholestatic liver injury in rats: Role of the hepatic stem cells. *Turk J Gastroenterol*. 28(6):476-484. doi: 10.5152/tjg.2017.16742.

Amanda, H., K. Angela, F. Emma, C. Katelyn, H. Greg, A. Emmanuella, B. Kevin, D. Emma, F. Mackenzie, F. Victoria, T.F. Philip, J. Kayla, M. Lisa, M. Jayasree, D.N. Mame, P. Connor, S. Yvonne, T. Aria, P.C. Christine. 2022. The behavioral effects of gestational and lactational benzo[a]pyrene exposure vary by sex and genotype in mice with differences at the Ahr and Cyp1a2 loci. *Neurotoxicology and Teratology*. Volume 89، 107056. oi.org/10.1016/j.ntt.2021.107056.

Banchroft, J.D., A. Stevens and D.R. Turner. 1996. Theory and Practice of Histological Techniques, Churchil livingstone, New York, London, San Francisco, Tokyo, Fourth edition.

Bektur Aykanat, N.E., S. Kacar, S. Karakaya and V. Sahinturk. 2020. Silymarin suppresses HepG2 hepatocarcinoma cell progression through downregulation of Slit-2/Robo-1 pathway. *Pharmacol. Rep* 72: 199–207 . doi.org/10.1007/s43440-019-00040-x.

Bhattacharya, S. 2011. Phytotherapeutic properties of milk thistle seeds: An overview. *Journal of Advanced Pharmacy Education & Research*, 1: 69–79.

Boei, J.J.W.A., S. Vermeulen, B. Klein, P.S. Hiemstra, R.M.Verhoosel, D.G.J. Jennen, A. Lahoz, H. Gmuender and H. Vrieling. 2017. Xenobiotic metabolism in differentiated human bronchial epithelial cells. *Arch Toxicol*. 91(5):2093-2105. doi: 10.1007/s00204-016-1868-7.

Bukowska, B. and P. Duchnowicz. 2022. Molecular mechanisms of action of selected substances involved in the reduction of benzo[a]pyrene-induced oxidative stress. Molecules 27:1379. doi: 10.3390/molecules27041379.

Bukowska, B., K. Mokra and J. Michałowicz. 2022. Benzo[*a*]pyrene-environmental occurrence, human exposure, and mechanisms of toxicity. *Int J* Mol Sci. 6; 23(11):6348. doi: 10.3390/ijms23116348.

Cichoż-Lach, H. and A. Michalak. 2014. Oxidative stress as a crucial factor in liver diseases. *World J Gastroenterol*. 20(25):8082-91. doi: 10.3748/wjg.v20.i25.8082.

Costa, J., M. Ferreira, L. Rey-Salgueiro and M.A. Reis-Henriques. 2011. Comparison of the waterborne and dietary routes of exposure on the effects of benzo(a)pyrene on biotransformation pathways in Nile tilapia (*Oreochromis niloticus*). *Chemosphere*. 84(10):1452-60. doi: 10.1016/j.chemosphere.2011.04.046.

Cui, Z., Y. Wang, L. Du and Y. Yu. 2022.Contamination level, sources, and health risk of polycyclic aromatic hydrocarbons in suburban vegetable field soils of Changchun, Northeast China. *Sci. Rep*. 12 (1), 11301. doi:10.1038/s41598-022-15285-5.

Dhatwalia, S.K., M. Kumar, P. Bhardwaj and D.K. Dhawan. 2019. White tea - A cost effective alternative to EGCG in fight against benzo(a)pyrene (BaP) induced lung toxicity in SD rats. *Food Chem Toxicol*. 131:110551. doi: 10.1016/j.fct.2019.05.059.

Dumludag, B., M.K. Derici, O. Sutcuoglu, B. Ogut, O.T. Pasaoglu, I.I. Gonul and U. Derici. 2022. Role of silymarin (Silybum marianum) in the prevention of colistin-induced acute nephrotoxicity in rats. *Drug Chem Toxicol.* 45(2):568-575. doi: 10.1080/01480545.2020.1733003.

Eldaly, E., M. Hussein, A. El-Gaml, D. El-hefny and M. Mishref. 2016. Polycyclic aromatic hydrocarbons (PAHs) in charcoal grilled meat (kebab) and kofta and the effect of marinating on their existence. *Zagazig Veterinary Journal*, 44(1): 40-47. doi: 10.21608/zvjz.2016.7830.

Elhassaneen, Y. 2000. Polycyclic aromatic hydrocarbons in foods: sources, occurrence, toxicological effects and therapy. Proceeding of the First Mansoura Conference of Food Science and Dairy Technology (17–19 October), Faculty of Agriculture, Mansoura University, Mansoura, Egypt. pp 319-341. [ISSN 1110-0346].

Elhassaneen, Y. 2004. The effect of charcoal broiled meat consumption on antioxidant defense system of erythrocytes and antioxidant vitamins in plasma. *Nutrition Research*, 24 (6): 435 - 446. doi:10.1016/j.nutres.2003.10.010.

Elhassaneen, Y. A. and El-Badawy, A. M. 2013. Influence of charcoal broiled meat consumption on the liver functions and non-enzymatic antioxidants in human blood. *Food and Nutrition Sciences*, 4 (1): 90 – 99. doi.org/ 10.4236/fns.2013.41013.

Elhassaneen, Y., H. Ghamry and L. Lotfy. 2018. Potential chemoprevention of liver disorders by dietary curcumin in rats treated with benzo(*a*)pyrene. Proceeding of the 1st Scientific International Conference of the Faculty of Specific Education, Minia University, "Specific Education, innovation and labor market" Minia, Egypt. doi:10.21608/JEDU.2018.105003.

Elhassaneen, Y., S. E. Hassab El-Nabi, A. I. Bayomi and A.R. ElKabary. 2022. Potential of watermelon (*citrullis lanatus*) peel extract in attenuating benzo[*a*]pyrene exposure-induced molecular damage in liver cells in vitro. *Journal of Biotechnology Research*, 8(3): 32-45. doi.org/10.32861/jbr.83.32.45.

Elhassaneen, Y., S. Sabry and B. Reham. 2016. Antioxidant activity of methanol extracts from various plant parts and their potential roles in protecting the liver disorders induced by benzo(*a*)pyrene. *Public Health International*, 2 (1): 38-50. Doi.org/ 10.11648/j.phi. 20170201.15.

Elhassaneen, Y.A. 1996. Biochemical and technological studies on pollution of fish with pesticides and polycyclic aromatic hydrocarbons. Ph.D. Thesis, Faculty of Agriculture, Mansoura University, Egypt.

Esteves, F., J. Rueff and M. Kranendonk. 2021.The central role of cytochrome P450 in xenobiotic metabolism-a brief review on a fascinating enzyme family. *J Xenobiot.* 22;11(3):94-114. doi: 10.3390/jox11030007.

European Commission. 2005. Commission recommendation 2005/208/EC of 4 February 2005 amending regulation (EC) no 466/2001 as regards polycyclic aromatic hydrocarbons. *Off J Eur Union* 2005; L34:3–5.

Fabiny, D.L. and G. Ertingshausen. 1971.Automated reaction-rate method for determination of serum creatinine with the CentrifiChem. *Clin Chem.* 17(8):696-700. PMID: 5562281.

Farida, T., O.A. Salawu, A.Y. Tijani and J.I. Ejiofor. 2012. Pharmacological evaluation of *Ipomea asarifolia* (Desr.) against carbon tetrachloride-induced hepatotoxicity in rats. *J. Ethnopharmacol.* 142: 642–646. doi: 10.1016/j.jep.2012.05.029.

Farkas, O., Jakus, J. and K. Héberger. 2004. Quantitative structure-antioxidant activity relationships of flavonoid compounds. *Molecules.* 9(12):1079-88. doi: 10.3390/91201079.

Feagins, L.A., A. Flores, C. Arriens, C. Park, T. Crook, A. Reimold and G. Brown. 2015. Nonalcoholic fatty liver disease: a potential consequence of tumor necrosis factor-inhibitor therapy. *Eur J Gastroenterol Hepatol.* 27(10):1154-60. doi: 10.1097/MEG.0000000000000421.

Federico. A., M. Dallio, G. DI Fabio, A. Zarrelli, S. Zappavigna, P. Stiuso, C. Tuccillo, M.Caraglia, C. Loguercio. 2015. Silybin-phosphatidylcholine complex protects human gastric and liver cells from oxidative stress. *In Vivo.* 29(5):569-75.

Fried, M.W., V.J. Navarro, N. Afdhal, S.H. Belle, A.S. Wahed, R.L. Hawke, E. Doo, C.M. Meyers and K.R. Reddy. 2012. Effect of silymarin (milk thistle) on liver disease in patients with chronic hepatitis C unsuccessfully treated with interferon therapy: a randomized controlled trial. *JAMA.* 18;308(3):274-82. doi: 10.1001/jama.2012.8265.

Fukuda, I., M. Tsutsui, I. Sakane and H. Ashida. 2009. Suppression of cytochrome P450 1A1 expression induced by 2,3,7,8-tetrachlorodibenzo-p-dioxin in mouse hepatoma hepa-1c1c7 cells treated with serum of (-)-epigallocatechin-3-gallate- and green tea extract-administered rats. *Biosci Biotechnol Biochem.* 73(5):1206-8. doi: 10.1271/bbb.80868.

Ghosh, J., A.R. Chowdhury, S. Srinivasan, M. Chattopadhyay, M. Bose, S. Bhattacharya, H. Raza, S.Y. Fuchs, A.K. Rustgi, F.J. Gonzalez and N.G. Avadhani. 2018.Cigarette smoke toxins-induced mitochondrial dysfunction and pancreatitis involves aryl hydrocarbon receptor mediated cyp1 gene expression: protective effects of resveratrol. *Toxicol Sci.* 166:428–40. doi: 10.1093/toxsci/kfy206.

Giannini, E.G., R. Testa and V. Savarino. 2005. Liver enzyme alteration: a guide for clinicians. *CMAJ.* 1;172(3):367-79. doi: 10.1503/cmaj.1040752.

Gillessen, A. and H.H. Schmidt. 2020. Silymarin as supportive treatment in liver diseases: a narrative review. *Adv Ther.* 37(4):1279-1301. doi: 10.1007/s12325-020-01251-y.

Gyurászová, M., R. Gurecká, J. Bábíčková and Ľ. Tóthová. 2020. Oxidative stress in the pathophysiology of kidney disease: implications for noninvasive monitoring and identification of biomarkers. *Oxid Med Cell Longev.* 2020:5478708. doi: 10.1155/2020/5478708.

Ha, K.B., W. Sangartit, A.R. Jeong, E.S. Lee, H.M. Kim, S. Shim. U. Kukongviriyapan, D.K. Kim, E.Y. Lee and C.H. Chung. 2022.Ew-7197 attenuates the progression of diabetic nephropathy in db/db mice through suppression of fibrogenesis and inflammation. *Endocrinol Metab* (Seoul) 37(1):96–111. doi: 10.3803/EnM.2021.1305.

Hajam, Y.A., R. Rani, S.Y. Ganie, T.A. Sheikh, D. Javaid, S.S. Qadri, S. Pramodh, A. Alsulimani, M.F. Alkhanani, S. Harakeh, A. Hussain, S. Haque and M.S. Reshi. 2022. Oxidative Stress in Human Pathology and Aging: Molecular Mechanisms and Perspectives. *Cells*, 11, 552. https://doi.org/10.3390/cells11030552.

Hodges, R.E. and D.M. Minich. 2015. Modulation of metabolic detoxification pathways using foods and food-derived components: a scientific review with clinical application. *J Nutr Metab*. 2015:760689. doi: 10.1155/2015/760689.

Jacques, C., E. Perdu, H. Duplan, E.L. Jamin, C. Canlet, L. Debrauwer, J.P. Cravedi, A. Mavon and D. Zalko. 2010. Disposition and biotransformation of 14C-benzo(a)pyrene in a pig ear skin model: ex vivo and in vitro approaches. *Toxicol Lett*. 10;199(1):22-33. doi: 10.1016/j.toxlet.2010.08.001.

Javeed, A., M. Ahmed, A. R. Sajid, A. Sikandar, M. Aslam, T.U. Hassan, Samiullah, Z. Nazir, M. Ji and C. Li. 2022. Comparative assessment of phytoconstituents, antioxidant activity and chemical analysis of different parts of milk thistle *Silybum marianum* L. *Molecules*. 20; 27(9):2641. doi: 10.3390/molecules27092641.

Jee, S.C., M. Kim and J.S. Sung. 2020b. Modulatory effects of silymarin on benzo[a]pyrene-induced hepatotoxicity. *Int J Mol Sci*. 30;21(7):2369. doi: 10.3390/ijms21072369.

Jee, S.C., M. Kim, K.S. Kim, H.S. Kim and J.S. Sung. 2020a. Protective effects of myricetin on benzo[a]pyrene-induced 8-hydroxy-2'-deoxyguanosine and BPDE-DNA adduct. *Antioxidants (Basel)*. 21;9(5):446. doi: 10.3390/antiox9050446.

Ji, K., C. Xing, F. Jiang, X. Wang, H. Guo, J. Nan, L. Qian, P. Yang, J. Lin, M. Li, J. Li, L. Liao and J. Tang. 2013. Benzo[a]pyrene induces oxidative stress and endothelial progenitor cell dysfunction via the activation of the NF-κB pathway. *Int J Mol Med*. 31(4):922-30. doi: 10.3892/ijmm.2013.1288.

Jiang, X.W., L. Qiao, X.X. Feng, L. Liu, Q.W. Wei, X.W. Wang and W.H. Yu. 2017. Rotenone induces nephrotoxicity in rats: oxidative damage and apoptosis. *Toxicol Mech Methods*. 27(7):528-536. doi: 10.1080/15376516.2017.1333553.

Jin, X., Q. Hua, Y. Liu, Z. Wu, D. Xu, Q. Ren and W. Zhao. 2021. Organ and tissue-specific distribution of selected polycyclic aromatic hydrocarbons (PAHs) in ApoE-KO mouse. *Environ Pollut*. 286:117219. 10.1016/j.envpol.2021.117219.

Khattab, S.A., W.F. Hussien, N. Raafat and E.A. Alaa El-Din. 2021.Modulatory effects of catechin hydrate on benzo[a]pyrene-induced nephrotoxicity in adult male albino rats. *Toxicol Res (Camb)*.17; 10(3):542-550. doi: 10.1093/toxres/tfab029.

Khazaei, R., A. Seidavi and M. Bouyeh. 2022. A review on the mechanisms of the effect of silymarin in milk thistle (*Silybum marianum*) on some laboratory animals. *Vet Med Sci*. 8(1):289-301. doi: 10.1002/vms3.641.

Kim, M., S.C. Jee, K.S. Kim, H.S. Kim, K.N. Yu and J.S. Sung. 2021. Quercetin and isorhamnetin attenuate benzo[a]pyrene-induced toxicity by modulating detoxification enzymes through the AhR and NRF2 signaling pathways. *Antioxidants*.10. 787. https://doi.org/10.3390/antiox10050787.

Kiruthiga, P.V., K. Karthikeyan, G. Archunan, S.K. Pandian and K.P. Devi. 2015. Silymarin prevents benzo(a)pyrene-induced toxicity in Wistar rats by modulating xenobiotic-metabolizing enzymes. *Toxicol Ind Health*. 31(6):523-41. doi: 10.1177/0748233713475524.

Kiruthiga, P.V., R.B. Shafreen, S.K. Pandian and K.P. Devi. 2007. Silymarin protection against major reactive oxygen species released by environmental toxins: exogenous H_2O_2 exposure in erythrocytes. *Basic Clin Pharmacol Toxicol*. 100(6):414-9. doi: 10.1111/j.1742-7843.2007.00069.x.

Korobkova, E.A. 2015. Effect of natural polyphenols on CYP metabolism: implications for diseases. *Chem Res Toxicol*. 28(7):1359-90. doi: 10.1021/acs.chemrestox.5b00121.

Kumar, M., G. Singh, P. Bhardwaj, S.K. Dhatwalia and D.K. Dhawan. 2017. Understanding the role of 3-O-Acetyl-11-keto-β-boswellic acid in conditions of oxidative-stress mediated hepatic dysfunction during benzo(a)pyrene induced toxicity. *Food Chem Toxicol*. 109(Pt 2):871-878. doi: 10.1016/j.fct.2017.03.058.

Kwon, D.Y., Y.S. Jung, S.J. Kim, Y.S. Kim, D.W. Choi. And Y.C. Kim.2013. Alterations in sulfur amino acid metabolism in mice treated with silymarin: a novel mechanism of its action involved in enhancement of the antioxidant defense in liver. *Planta Med*. (12):997-1002. doi: 10.1055/s-0032-1328704.

Li, C.C., C.Y. Hsiang, S.L. Wu. and T.Y. Ho. 2012. Identification of novel mechanisms of silymarin on the carbon tetrachloride-induced liver fibrosis in mice by nuclear factor-kappaB bioluminescent imagingguided transcriptomic analysis. *Food Chem Toxicol*. 50(5):1568–75. https://doi.org/10.1016/j.fct.2012.02.025.

Li, S., H.Y. Tan, N. Wang, Z.J. Zhang, L. Lao, C.W. Wong. and Y. Feng. 2015. The role of oxidative stress and antioxidants in liver diseases. *Int J Mol Sci*. 16(11):26087-124. doi: 10.3390/ijms161125942.

Lv, W., G.W. Booz, F. Fan, Y. Wang and R.J. Roman. 2018. Oxidative stress and renal fibrosis: recent insights for the development of novel therapeutic strategies. *Front Physiol*. 16;9:105. doi: 10.3389/fphys.2018.00105.

Mahran, M.Z. and Y.A.Elhassaneen. 2023a. Attenuation of benzo[*a*]pyrene-induced oxidative stress and cell apoptosis in albino rats by wild milk thistle (*Silybum Marianum* L.) seeds extract. *Egyptian J. of Chemistry*, 66(13):1671-1687. doi: 10.21608/ejchem.2023.214010.8042.

Mahran, M.Z. and Y.A. Elhassaneen. 2023b. A study of the physical, chemical, phytochemical and nutritional properties of wild *Silybum marianum* L. seeds oil to investigate its potential use to boost edible oil self-sufficiency in Egypt. *Alex. Sci. Exch. J.*, 44(1): 81-91. doi: 10.21608/asejaiqjsae.2023.292950.

Mahran, M.Z., G.M. Elbassyouny and Y. A. Elhassaneen. 2018. Preventive effects of onion skin powder against hepatotoxicity in rats treated with benzo(*a*)pyrene." In Proceeding of the Annual Conference (13th Arab; 10th International), 11-12 April, Faculty of Specific Education, Mansoura University, Mansoura, Egypt. Higher Education in Egypt and the Arab World in the Light of Sustainable Development Strategies.

Malkani, N., A. Naeem, F. Ijaz, S. Mumtaz, S. Ashraf and M.I. Sohail. 2020. Silybum marianum (milk thistle) improves vancomycin induced nephrotoxicity by downregulating apoptosis. *Mol Biol Rep*. 47(7):5451-5459. doi: 10.1007/s11033-020-05635-9.

Mee-Young, L., S. Chang-Seob, S. In-Shik, K. Young-Bum, K. Jung-Hoon. and S. Hyeun-Kyoo. 2013. Evaluation of oral subchronic toxicity of soshiho-tang water extract: the traditional herbal formula in rats. *Evidence-Based Complementary and Alternative Medicine*, . Article ID 590181, 9 . https://doi.org/10.1155/2013/590181.

Mojiri, A., J.L. Zhou, A. Ohashi, N. Ozaki and T. Kindaichi. 2019. Comprehensive review of polycyclic aromatic hydrocarbons in water sources, their effects and treatments. *Sci. Total Environ*. 2019:133971. doi: 10.1016/j.scitotenv.2019.133971.

Murawska-Ciałowicz, E., Z. Jethon, J. Magdalan, L. Januszewska, M. Podhorska-Okołów, M. Zawadzki, T. Sozański and P. Dzięgiel. 2011. Effects of melatonin on lipid peroxidation and antioxidative enzyme activities in the liver, kidneys and brain of rats administered with benzo(a)pyrene. *Exp Toxicol Pathol*. 63(1-2):97-103. doi: 10.1016/j.etp.2009.10.002.

Murray, I.A., A.D. Patterson and G.H. Perdew. 2014. Aryl hydrocarbon receptor ligands in cancer: friend and foe. *Nat Rev Cancer*. 14(12):801-14. doi: 10.1038/nrc3846.

Nabavi, S.M., S.F. Nabavi, A.M. Latifi, A.H. Moghaddam and C. Hellio. 2012. Neuroprotective effects of silymarin on sodium fluoride-induced oxidative stress. *J. of Fluorine Chemistry*. 142: 79–82. doi.org/10.1016/j.jfluchem.2012.06.029.

Nanez, A., I.N. Ramos, K.S. Ramos. 2001. A mutant Ahr allele protects the embryonic kidney from hydrocarbon-induced deficits in fetal programming. *Environ Health Perspect*. 119(12):1745-53. doi: 10.1289/ehp.1103692.

Nencini, C., G. Giorgi and L. Micheli. 2007. Protective effect of silymarin on oxidative stress in rat brain. *Phytomedicine*. 14(2-3):129-35. doi: 10.1016/j.phymed.2006.02.005.

Ogbonna, C.U., C.O. Ujowundu, G.N. Okwu, A.A. Emejulu, C.S. Alisi and K.O. Igwe. 2016. Biochemical and histological evaluation of benzo[a]pyrene induced nephrotoxicity and therapeutic potentials of *Combretum zenkeri* leaf extract. *African J Pharmacy and Pharmacol.*10: 873–82.

Omura, T. and R. Sato. 1964.The carbon monoxide-binding pigment of liver microsomes. II. Solubilization, purification, and properties. *J biol chem*. 239:2379-85.

Ortiz-Delgado, J.B., A. Behrens, H. Segner and C. Sarasquete. 2008. Tissue-specific induction of EROD activity and CYP1A protein in *Sparus aurata* exposed to B(a)P and TCDD. *Ecotoxicol Environ Saf*. 69(1):80-8. doi: 10.1016/j.ecoenv.2006.12.021.

Ou, Q., Y. Weng, S. Wang, Y. Zhao, F. Zhang, J. Zhou and X. Wu. 2018. Silybin alleviates hepatic steatosis and fibrosis in NASH mice by inhibiting oxidative stress and involvement with the Nf-κB pathway. *Dig Dis Sci*. 63(12):3398-3408. doi: 10.1007/s10620-018-5268-0 .

Owumi, S.E., G. Adeniyi and A.K. Oyelere. 2021. The modulatory effect of taurine on benzo (a) pyrene-induced hepatorenal toxicity. *Toxicol Res (Camb)*. 12;10(3):389-398. doi: 10.1093/toxres/tfab016.

Paltanaviciene, A., D. Zabulyte, J. Kalibatas, and S. Uleckiene. 2007. Evaluation of the combined effect of cadmium, benzo(a)pyrene, and pyrene in general toxicity studies on Wistar rats. *Medycyna Weterynaryjna*. 63 (1):51–5.

Parasuraman, S., R. Raveendran and R. Kesavan. 2010. Blood sample collection in small laboratory animals. J Pharmacol Pharmacother. 1(2):87-93. doi: 10.4103/0976-500X.72350.

Patel, A.B., S. Shaikh, K.R. Jain, C. Desai and D. Madamwar. 2020.Polycyclic aromatic hydrocarbons: sources, toxicity, and remediation approaches. *Front Microbiol*. 5;11:562813. doi: 10.3389/fmicb.2020.562813.

Polyak, S.J., C. Morishima, V. Lohmann, S. Pal, D.Y. Lee, Y. Liu, T.N. Graf and N.H. Oberlies. 2010. Identification of hepatoprotective flavonolignans from silymarin. *Proc Natl Acad Sci U S A*. 30;107(13):5995-9. doi: 10.1073/pnas.0914009107.

Prabu, S.M. and M. Muthumani. 2021. Retraction Note to: Silibinin ameliorates arsenic induced nephrotoxicity by abrogation of oxidative stress, inflammation and apoptosis in rats. *Mol Biol Rep*. 48(6):5377. doi: 10.1007/s11033-021-06475-x.

Rangi, S., S.K. Dhatwalia, P. Bhardwaj, M. Kumar and D.K. Dhawan. 2018. Evidence of similar protective effects afforded by white tea and its active component 'EGCG' on oxidative-stress mediated hepatic dysfunction during benzo(a)pyrene induced toxicity. *Food Chem Toxicol*. 116(Pt B):281-291. doi: 10.1016/j.fct.2018.04.044.

Reeves, P.G., F.H. Nielsen and G.C. Fahey.1993. AIN-93 Purified Diets for Laboratory Rodents: Final Report of the American Institute of Nutrition Ad Hoc Writing Committee on the Reformulation of the AIN-76A Rodent Diet. *The J. of Nutrition*, 123(11):1939–1951. doi:10.1093/jn/123.11.1939.

Reuter, S., S.C. Gupta, M.M. Chaturvedi and B.B. Aggarwal. 2010. Oxidative stress, inflammation and cancer: how are they linked? *Free Radic Biol Med*. 49:1603–16. doi: 10.1016/j.freeradbiomed.2010.09.

Ross, S.M. 2008. Milk thistle (*Silybum marianum*): an ancient botanical medicine for modern times. *Holist Nurs Pract*. 22(5):299-300. doi: 10.1097/01.HNP.0000334924.77174.6d.

Roy, S. and S. Bhattacharya. 2006. Arsenic-induced histopathology and synthesis of stress proteins in liver and kidney of *Channa punctatus*. *Ecotoxicology and Environmental Safety*, 65(2): 218–229. doi:10.1016/j.ecoenv.2005.07.005.

Sánchez-Valle, V., N.C. Chávez-Tapia, M. Uribe and N. Méndez-Sánchez. 2012. Role of oxidative stress and molecular changes in liver fibrosis: a review. *Curr Med Chem*. (28):4850-60. doi: 10.2174/092986712803341520.

Shahid, A., R. Ali, N. Ali, S.K. Hasan, P. Bernwal, S.M. Afzal, A.Vafa and S. Sultana. 2016b. Modulatory effects of catechin hydrate against genotoxicity, oxidative stress, inflammation and apoptosis induced by benzo(a)pyrene in mice. *Food and Chemical Toxicology*, 92, 64–74. doi:10.1016/j.fct.2016.03.021.

Shahid, A., R. Ali, N. Ali, S. K. Hasan, S. Rashid, F. Majed and S. Sultana. 2016a. "Attenuation of genotoxicity, oxidative stress, apoptosis and inflammation by rutin in benzo(a)pyrene exposed lungs of mice: plausible role of NF-κB, TNF-α and Bcl-2" *Journal of Complementary and Integrative Medicine*, vol. 13, no. 1, pp. 17-29. doi.org/10.1515/jcim-2015-0078.

Sinha, M. and D. Dash. 2018. Mangiferin protects renal impairment against benzo(a)pyrene induced toxicity by regulating mitochondrial and DNA integrity. *Journal of Drug Delivery and Therapeutics*, 8(1), 92-97. doi.org/10.22270/jddt.v8i1.1541.

Sivanagi R.T., S.K. Prasanna, P. Nirmala and C.S. Shastry. 2012. Biochemical studies on hepato and nephroprotective effect of butterfly tree (*Bauhinia purpurealinn*.) against acetaminophen induced toxicity. *International Journal of Research in Ayurveda & Pharmacy*. 3:455–60.

Soleimani, V., P.S. Delghandi, S.A. Moallem and G. Karimi. 2019. Safety and toxicity of silymarin, the major constituent of milk thistle extract: An updated review. *Phytother Res*. 33(6):1627-1638. doi: 10.1002/ptr.6361.

Stolf, A.M., C.C. Cardoso and A. Acco. 2017. Effects of silymarin on diabetes mellitus complications: A Review. *Phytother Res*. 31(3):366-374. doi: 10.1002/ptr.5768.

Sun, K., X. Tang, S. Song, Y. Gao, H. Yu, N. Sun, B. Wen and C. Mei. 2021. Hyperoxalemia leads to oxidative stress in endothelial cells and mice with chronic kidney disease. *Kidney Blood Press Res*. 46(3):377–86. doi: 10.1159/000516013.

Surai, P.F. 2015. Silymarin as a natural antioxidant: an overview of the current evidence and perspectives. *Antioxidants (Basel)*. 20;4(1):204-47. doi: 10.3390/antiox4010204.

Tabacco, A., F. Meiattini, E. Moda and P. Tarli. 1979.Simplified enzymic/colorimetric serum urea nitrogen determination. *Clin Chem*. 25(2):336-7. PMID: 759035.

Tête, A., I. Gallais, M. Imran, M. Chevanne, M. Liamin, L. Sparfel, S. Bucher, A. Burel, N. Podechard, B.M.R. Appenzeller, B. Fromenty, N. Grova. O. Sergent and D. Lagadic-Gossmann. 2018. Mechanisms involved in the death of steatotic WIF-B9 hepatocytes co-exposed to benzo[a]pyrene and ethanol: a possible key role for xenobiotic metabolism and nitric oxide. *Free Radic Biol Med*. 129:323-337. doi: 10.1016/j.freeradbiomed.2018.09.042.

Thapa, B.R. and A. Walia. 2007. Liver function tests and their interpretation. *Indian J Pediatr*. 74, 663–671. https://doi.org/10.1007/s12098-007-0118-7.

Tietz, N. M. 1994. Fundamentals of Clinical Chemistry. 2nd Edn WB Saunders, Philadelphia. pp: 692.

Tutun, B., H. Elbe, N. Vardi, H. Parlakpinar, A. Polat, M. Gunaltili, M.M. Guclu and E.N. Yasar. 2019. Dexpanthenol reduces diabetic nephropathy and renal oxidative stress in rats. *Biotech Histochem*. 94(2):84-91. doi: 10.1080/10520295.2018.1508746.

Uno, S., T.P. Dalton, S. Derkenne, C.P. Curran, M.L. Miller, H.G. Shertzer and D.W. Nebert. 2001. Oral exposure to benzo[a]pyrene in the mouse: detoxication by inducible cytochrome P450 is more important than metabolic activation. *Mol Pharmacol*. 65(5):1225-37. doi: 10.1124/mol.65.5.1225.

Vassault, A., D. Grafmeyer, J. Graeve, R. Cohen, A. Beaudonnet and J. Bienvenu. 1999. Quality specifications and allowable standards for validation of methods used in clinical biochemistry. *Ann Biol Clin* (Paris), 57(6): 685-95.

Vermillion Maier, M.L., L.K. Siddens, J.M. Pennington, S.L. Uesugi, K.A. Anderson. L.G. Tidwell. S.C. Tilton. T.J. Ognibene, K.W. Turteltaub, J.N. Smith and D.E. Williams. 2022. Benzo[a]pyrene (BaP) metabolites predominant in human plasma following escalating oral micro-dosing with [^{14}C]-BaP. *Environ Int*. 15; 159:107045. doi: 10.1016/j.envint.2021.107045.

Voumik, L.C. and T. Sultana. 2022. Impact of urbanization, industrialization, electrification and renewable energy on the environment in BRICS: fresh evidence from novel CS-ARDL model. Heliyon. 7;8(11):e11457. doi: 10.1016/j.heliyon.2022.e11457.

Wang, X. Z. Zhang and S.C. Wu. 2020. Health benefits of silybum marianum: phytochemistry, pharmacology, and applications. *J Agric Food Chem*. 21;68(42):11644-11664. doi: 10.1021/acs.jafc.0c04791.

Wang, Y.H., W.Y. Wang, C.C. Chang, K.T. Liou, Y.J. Sung, J.F. Liao, C.F. Chen, S. Chang, Y.C. Hou, Y.C. Chou and Y.C. Shen. 2006. Taxifolin ameliorates cerebral ischemia-reperfusion injury in rats through its anti-oxidative effect and modulation of NF-kappa B activation. *J Biomed Sci*. 13(1):127-41. doi: 10.1007/s11373-005-9031-0.

Welz, A.N., A. Emberger-Klein and K. Menrad. 2018. Why people use herbal medicine: insights from a focus-group study in Germany. *BMC Complement Altern Med*. 15;18(1):92. doi: 10.1186/s12906-018-2160-6.

Wu, X., W. Sun, B. Huai, L. Wang, C. Han, Y. Wang and W. Mi. 2023.Seasonal variation and sources of atmospheric polycyclic aromatic hydrocarbons in a background site on the Tibetan Plateau. *J. Environ. Sci*., 125 pp. 524-532, 10.1016/J.JES.2022.02.042.

Zhao, H., L. Chen, T.Yang, Y. Feng, N. D. Vaziri, B. Liu, Q. Liu, Y. Guo and Y. Zhao. 2019.Aryl hydrocarbon receptor activation mediates kidney disease and renal cell

carcinoma. *J Transl Med.* 17, 302. doi.org/10.1186/s12967-019-2054-5.

الملخص العربي

التأثيرات الوقائية المحتملة لبذور شوك الحليب ضد الإصابات الكبدية والكلوية الناجمة عن البنزو[أ]بيرين في الفئران: دراسات بيوكيميائية وهستوباثولوجية

يوسف عبد العزيز الحسانين ، محمد زكريا مهران

يشكل البنزو[أ]بيرين، وهو هيدروكربون عطري متعدد الحلقات، تهديدا كبيرا لصحة الإنسان باعتباره ملوثا بيئيا ومنقولا بالغذاء منتشرا بشكل متزايد. كشفت دراستنا السابقة أن المستخلص الإيثانولي لبذور شوك الحليب البري (SMSE) يخفف من الإجهاد التأكسدي الناجم عن البنزو[أ]بيرين وموت الخلايا المبرمج في الفئران البيضاء. في هذا العمل، قمنا بتوسيع فرضيتنا لدراسة التأثيرات الوقائية المحتملة لـ SMSE ضد الإصابات الكبدية والكلوية الناجمة عن البنزو[أ]بيرين. تم تقسيم ستة وثلاثين فأر ألبينو ذكر إلى ست مجموعات: المجموعة الأولى، المجموعة الضابطة السالبة، تلقت ١٠مل/كجم/من وزن الجسم من زيت الذرة مرتين أسبوعيا عن طريق الفم؛ أعطيت المجموعة الثانية، المجموعة الضابطة الموجبة، ٥٠ ملجم/كجم/من وزن الجسم من البنزو[أ]بيرين مذاب في زيت الذرة مرتين أسبوعيا، وتم إعطاء المجموعات الثالثة، الرابعة، الخامسة، والسادسة البنزو[أ]بيرين + SMSE بجرعات ٢٠٠، ٤٠٠، ٦٠٠، و٨٠٠ ملجم/كجم/يوم، على التوالي، عن طريق الفم لمدة أربعة أسابيع. أدى التعرض للبنزو[أ]بيرين إلى زيادة ملحوظة ($p \leq 0.05$) في الأوزان النسبية للكبد بنسبة (٣٣,٣٣%) والكلى (٣٩,٦٨%)؛ نشاط انزيمات السيتوكروم (CYP450)،

مؤشر للتحولات الحيوية، (٦٨,٢٥%)؛ مستويات عامل نخر الورم ألفا (TNF-α)، وسيط مسبب للالتهابات، (٩٥,٩٥%)؛ أنشطة إنزيمات الكبد (AST، ١٢٤,٠٩%، ALT، ١٢٤,٩٨%، وALP، ١٢٨,٧٧%)؛ ومؤشرات وظائف الكلى (اليوريا ٦٠,١٨%، والكرياتينين ٦٨,٣٥% في الدم)، مصحوبة بتغيرات نسيجية مرضية شديدة في أنسجة الكبد والكلى مقارنة بالمجموعة الضابطة السالبة. على العكس من ذلك، أدت تدخلات SMSE بشكل ملحوظ إلى خفض المعدلات المرتفعة لهذه المؤشرات اعتمادا على الجرعة مع تحسين البنية النسيجية للكبد والكليتين. قد تنجم التأثيرات الوقائية لـ SMSE لإحتوائه على المركبات النشطة بيولوجيا التي تعمل على تنظيم الإنزيمات الأيضية للبنزو[أ]بيرين، تثبيط نشاط انزيمات CYP450، قمع TNF-α، والتخلص من المركبات الوسيطة التفاعلية الأخرى. تشير نتائجنا إلى أن SMSE نهج طبيعي محتمل للتخفيف من الآثار الضارة للملوثات البيئية ويستحق المزيد من البحث.

الكلمات المفتاحية: بذور شوك الحليب، بنزو[أ]بيرين، السمية الكبدية، السمية الكلوية، السيتوكروم P450، الاستجابة الالتهابية، هستوباثولوجي.